Surface Quality and Geometric Accuracy Control of Fuel Nozzle Single-Pass Honing

Changyong Yang (yangchy@nuaa.edu.cn)
Nanjing University of Aeronautics & Astronautics

Hao Su
anjing University of Aeronautics and Astronautics

Shaowu Gao
anjing University of Aeronautics and Astronautics

Yucan Fu
anjing University of Aeronautics and Astronautics

Wenfeng Ding
anjing University of Aeronautics and Astronautics

Jiuhua Xu
anjing University of Aeronautics and Astronautics

Original Research

Keywords: Surface roughness, Geometric accuracy, Single-pass honing, Cutting force

Posted Date: February 4th, 2021

DOI: https://doi.org/10.21203/rs.3.rs-168419/v1

Version of Record: A version of this preprint was published at The International Journal of Advanced Manufacturing Technology on April 24th, 2021. See the published version at https://doi.org/10.1007/s00170-021-07103-5.

Surface quality and geometric accuracy control of fuel nozzle single-pass honing

Changyong Yang[1] · Hao Su[1] · Shaowu Gao[1] · Yucan Fu[1] · Wenfeng Ding[1] · Jiuhua Xu[1]

1 College of Mechanical and Electrical Engineering, Nanjing University of Aeronautics and Astronautics, Nanjing 210016, People's Republic of China

Corresponding author: Changyong Yang, yangchy@nuaa.edu.cn

Abstract

Surface quality and geometric accuracy are important evaluation indexes for machining quality of parts. In order to realize the quality control of nozzle honing, it is necessary to clarify the influence of honing parameters on surface roughness, dimension accuracy and shape accuracy. Cutting force is an important process parameter, which has an important influence on machining quality. The research on the influence of honing parameters on cutting force contributes to explain the honing process and the influence of honing parameters on machining quality. Therefore, the cutting force during honing was analyzed and modeled, and the influence of honing parameters on cutting force was clarified, and then the influence law of honing parameters on surface roughness, bore diameter and shape accuracy was explored. Finally, according to the processing requirements of fuel nozzles, the honing process optimization was carried out and the optimal processing parameters were obtained.

Keywords Surface roughness; Geometric accuracy; Single-pass honing; Cutting force

1 Introduction

Fuel nozzle is a key unit of aero-engines, which directly affects aero-engine performance [1]. The atomization of fuel nozzle is affected by the surface roughness and geometric accuracy of hole [2,3]. Poor surface roughness results in the fluctuation of flow, especially the deviation is large when rate of flow is small. Therefore, the surface roughness is extremely an important evaluation index of quality. Besides, poor geometric accuracy will not only affect the stability of fuel flow, but also affect the uniformity of fuel atomization.

A novel super-abrasive tool of fixed dimension has been employed in single-pass honing. When the tool rotates, the tool passes through the hole to remove some material at the same time [4-6]. Combining the advantages of reaming and honing, single-pass honing is a kind of abrasive process, which can achieve higher dimension consistency and shape accuracy and have been widely used in the finish processing of holes in the hydraulic field [7, 8]. The processing capacity of single-pass honing is perfectly matched with the requirements of fuel nozzles, which has great application potential in high efficiency and high consistency machining of nozzles.

In order to fully tap the potential of honing process and improve the efficiency and quality of single-pass honing, a lot of work has been carried out. Arunachalam designed the orthogonal test, and systematically studied the influence of honing process parameters, including spindle speed, feed speed, removal allowance, abrasive particle size, workpiece material, fixture and tool length, on the cylindricity and surface roughness of single-pass honed hole [9]. It is pointed out that most of the workpiece materials in honing are removed by ploughing of grains. The orthogonal test of single-pass honing for steering gear valve sleeve was carried out [10]. The results showed that the spindle speed and feed speed were the decisive factors of roundness, while the surface roughness mainly depended on the particle size. The straightness of the hole was determined by the positioning accuracy of the machine tool and the fixture system. Through a series of honing process tests, the influence of honing parameters and workpiece material on tool wear and machining accuracy was established, and the selection principle of honing tool and process parameters was given [11]. The machining parts of the above research are all holes larger than 10 mm, and the honing tool has good rigidity, which is different from the fuel injection nozzle processing with small bore diameter.

The diameter of fuel nozzle is generally less than 1 mm, so the diameter of the honing tool used is smaller. In the early stage, a series of studies have been carried out on the preparation and life prediction of small diameter flexible honing tools [12]. The diameter of the honing tool is small, which rigidity is poor. Single-pass honing is a kind of flexible machining, which is quite different from that of the honing tool with better rigidity. Therefore, it is necessary to study the surface quality and geometric accuracy of honed hole for flexible honing tool. In this paper, the surface quality and geometric accuracy of single-pass honing are made a profound study, combining the axial force and torque of honing process parameters. Finally, taking the surface quality and geometric accuracy as the optimization objects, the appropriate honing parameters are determined to realize the high-

efficiency and precision machining of fuel nozzle.

2 Experimental Procedures

As shown in Fig. 1, the test was carried out on machining center produced by DMG MORI. The maximum speed of the spindle is 42,000 rpm, and the runout is within 5 μm. The workpiece material is 4Cr13 with HRC55 after heat treatment. The diameter and length of original holes were from 0.744 to 0.750 mm and 1.5 mm obtained by drilling and reaming respectively. The single-pass honing tool was dressed, which had 270/325 mesh electroplated CBN grains. The maximum profile obtained by simulation is distributed along the axial direction as shown in Fig. 2. The Kistler 9272 dynamometer was used to measure the axial force and torque during single-pass honing. The high-precision compound CMM produced by Werth was used to measure the bore diameter. The honed hole was cut along the axis, and the machined surface morphology and surface roughness was observed by Sensofar. The factors and levels were shown in table 1.

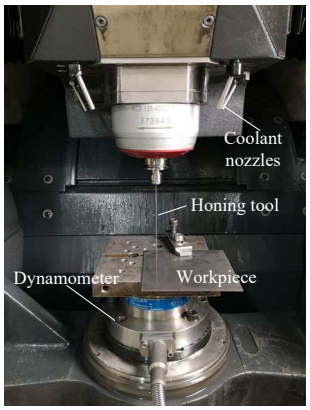

Fig. 1 Single-pass honing platform

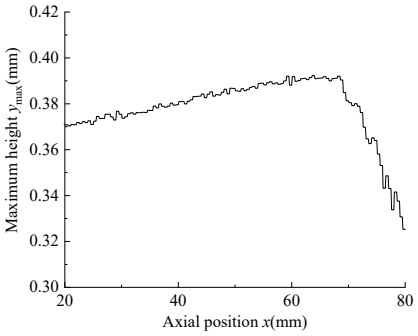

Fig. 2 Maximum contour distribution of tool

Table 1 Experimental conditions

Factors	Levels
Spindle speed (rpm)	2000，3000，4000，5000
Feedrate (mm/min)	20，30，40，50，60，70，80，90，100
Retracting speed (mm/min)	10，20，30，40，50，60，100，150，200，500

3 Analysis of cutting force

Force is an important process parameter during hole machining, which directly reflects the interaction between tool and workpiece, and the stability of the machining process. Through the analysis of micro cutting process, the cutting force model in single-pass honing was established. On this basis, the influence of process parameters and tool profile on cutting force was analyzed.

3.1 Modeling of axial force and torque

During single-pass honing, the relative position and contact state of tool and workpiece change all the time, and the micro cutting load at each position of tool is also different. Therefore, in order

to calculate the change of cutting force with time, it is necessary to define the micro cutting load at each position of the single-pass honing tool. The force analysis diagram of single abrasive is shown in Fig. 3. The material deformation resistance and friction force of a single abrasive due to the main cutting motion can be divided into tangential force F_{st} along the main cutting speed direction and normal force F_{sn} along the radial direction. In addition, the feed resistance force caused by the tool axial feed movement along the hole axis is recorded as the axial force F_{sa}. The cutting force of a single abrasive is approximately proportional to the undeformed chip cross-sectional area A_{cs} [13,14]:

$$F_{st} = k_t A_{cs} \tag{1}$$

$$F_{sn} = k_n A_{cs} \tag{2}$$

$$F_{sa} = k_a A_{cs} \tag{3}$$

where k_t, k_n and k_a are cutting coefficients, which depend on the material properties and the grain morphology. During single-pass honing, the relative position of tool and workpiece is shown in Fig. 4. If $t = 0$, the tool overlaps with the left end of the workpiece at $x = 0$. When the axial feed rate is v_a, the position $x(t)$ of the workpiece left end in the tool axis can be expressed as

$$x(t) = v_a t \tag{4}$$

At a certain time t, the tool at axial section $[x(t), x(t)+L]$ contacts the workpiece with length L. Assuming that the cutting force coefficients of different effective grains on the tool surface are the same, the axial force and torque can be expressed as

$$F_a(t) = \int_{x(t)}^{x(t)+L} k_a A_{cs} dx = k_a A_c(t) \tag{5}$$

$$M_a(t) = \int_{x(t)}^{x(t)+L} k_t A_{cs} r_t dx = k_t r_t A_c(t) \tag{6}$$

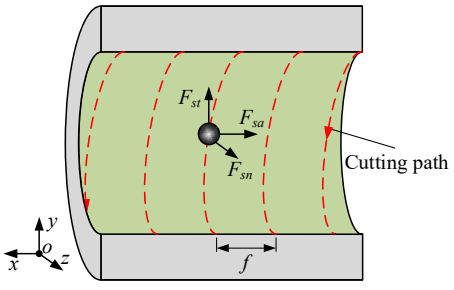

Fig. 3 The force diagram of single grain

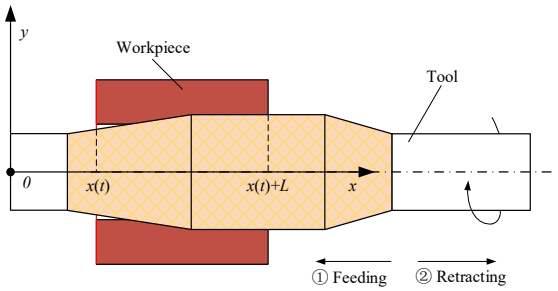

Fig. 4 The relative position of tool and workpiece

where $A_c(t)$ is the sum of the undeformed chip cross-sectional area that the effective grains contact the workpiece at time t, which can be expressed as

$$A_c(t) = \frac{\Delta V_u(t)}{s_L} \tag{7}$$

where $\Delta V_u(t)$ the sum of the undeformed chip volume that the effective grains contact the workpiece at time t, and S_L is the cutting distance of a single abrasive on the workpiece surface, which can be expressed as

$$s_L = \frac{L}{\sin\alpha} \tag{8}$$

where α is an angle between the direction of cutting speed and the tangential direction of hole.

The tool is discretized along the axial direction with the interval of l = 0.5 mm. The undeformed chip volume on each segment of the tool is calculated respectively. Under the condition that the bearing ratio distribution of the tool in the current wear state and the bearing ratio of the workpiece in the initial state are known, the undeformed chip volume on the segment i of the tool can be expressed as [15]

$$\Delta V_{ui} = \pi d_t L \int_{y_{wi}}^{y_{maxi}} T_{di}(y) W_i(y) dy \tag{9}$$

Therefore, $\Delta V_u(t)$ can be expressed as the sum of the undeformed chip volume that the tool contacts the workpiece at time t.

$$\Delta V_u(t) = \sum \Delta V_{ui} \tag{10}$$

According to the test, the workpiece length L = 1.5 mm, which is 3 times of the tool discrete interval l. Therefore, at discrete time t, $\Delta V_u(t)$ can be expressed as

$$\Delta V_u(t) = \Delta V_{ui} + \Delta V_{u(i+1)} + \Delta V_{u(i+2)} \tag{11}$$

where i satisfies

$$i = \frac{x(t)}{l} + 1 \tag{12}$$

3.2 Influence of machining parameters on cutting force

When the tool speed n=5000 rpm, the feed rate per revolution f=0.01 mm/r, and the chip forming coefficient k_p=0.1, the variation of axial force $F_a(t)$ measured by test and the sectional area $A_c(t)$ of undeformed chip by theory calculation with time are shown in Fig. 5 (a). With the honing process, $F_a(t)$ and $A_c(t)$ firstly increase and then decrease, showing a good consistency in the change trend.

In the honing process, the lowest point of the workpiece surface, y_w, firstly interferes with the tool, as shown in Fig. 6. Due to the influence of surface roughness and cylindricity error of workpiece surface, the bearing ratio at the first cutting position of workpiece surface is small, and the cutting load of tool is also small. With single-pass honing, the cutting layer height increases, and the bearing ratio of the workpiece at the cutting position increases gradually, which leads to the increase of the cutting load. When the finishing part starts cutting the workpiece, the bearing ratio

of the workpiece gradually decreases, resulting in the reduction of cutting load. Therefore, the axial force and undeformed chip cross-sectional area increase first and then decrease. It can be seen from Fig. 2 that the maximum contour of the tool is not smooth. When the height of the tool contour increases suddenly, the cutting load will increase suddenly, which leads $A_c(t)$ appearing a peak value. On the contrary, when the tool contour height suddenly decreases, $A_c(t)$ will appear a valley value. The peak valley of $A_c(t)$ is basically synchronous with that of $F_a(t)$, as shown in Fig. 5(a).

When f = 0.02 mm/r, the variation of $F_a(t)$ and $A_c(t)$ with time are shown in Fig. 5(b). Compared Fig. 5(b) with Fig. 5(a), the values of $F_a(t)$ and $A_c(t)$ increase significantly when f is increased. To sum up, $A_c(t)$ calculated by simulation can better reflect cutting force in the actual honing process. Therefore, in the follow-up analysis, the influence of honing parameters on $A_c(t)$ will be studied, and then the influence of honing parameters on cutting force will be revealed.

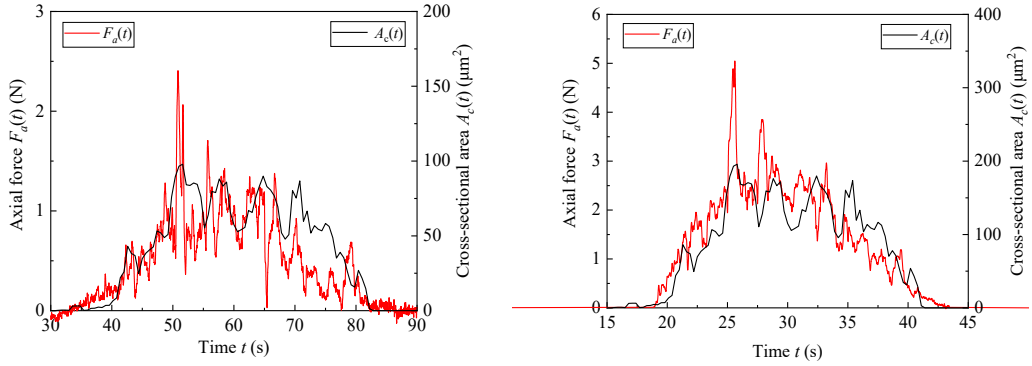

(a) f=0.01 mm/r (b) f=0.02 mm/r

Fig. 5 Measured $F_a(t)$ and calculated $A_c(t)$ under different f

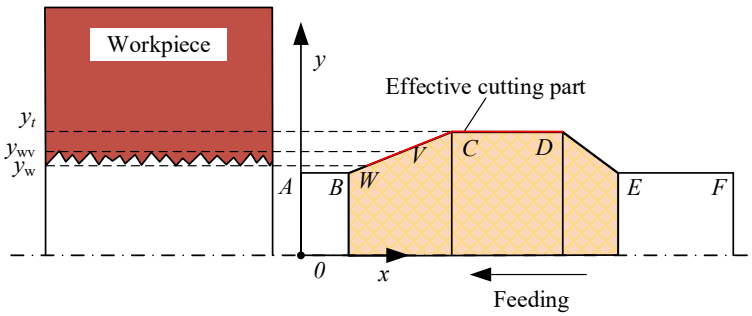

Fig. 6 Contact diagram of micro contour between tool and workpiece

When tool speed is 5000 rpm and initial bore diameter is 0.75 mm, $A_c(t)$ under different f is shown in Fig. 7. With the increase of f, the honing time is shortened, thus $A_c(t)$ is significantly increased. When f increases from 0.005 mm/r to 0.02 mm/r, the maximum value of $A_c(t)$ increases from 48.96 μm² to 195.8 μm². The cutting distance s_L of a single grain decreases with the increase of f, while the undeformed chip volume changes little. Therefore, it can be considered that the axial force and torque in single-pass honing process will increase significantly with the increase of f.

When tool speed is 5000 rpm and feedrate per revolution f is 0.01 mm/r, $A_c(t)$ under different initial bore dimeter is shown in Fig. 8. Because of the taper structure of the tool cutting part, the length of the tool actual effective cutting part decreases with the increase of bore diameter, and the contact time between the tool and the workpiece is delayed. When the initial bore diameter is increased, $A_c(t)$ decreases significantly, which can decrease cutting force effectively.

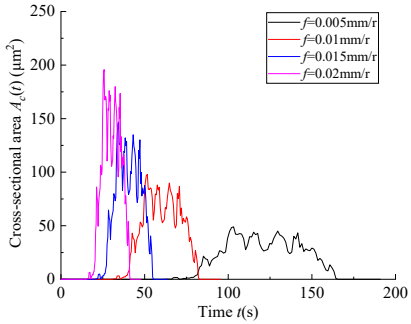

Fig. 7 Influence of f on $A_c(t)$

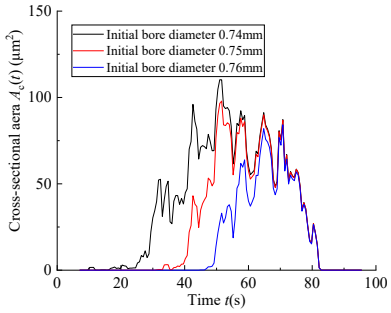

Fig. 8 Influence of initial bore diameter on $A_c(t)$

3.3 Influence of tool contour on cutting force

The tool contour effects the axial distribution of $A_c(t)$ in honing process, and then effects cutting force. In order to study the influence of different tool contours on cutting force, the contour of different stages of tool dressing is taken. Under the conditions of tool speed n=5000 rpm and feedrate per revolution f=0.01 mm/r, $A_c(t)$ is calculated respectively, as shown in Fig. 9. With the dressing of the tool, the cutting load at the front end of the tool decreases significantly, the peak value of the cutting load at the tool end decreases and becomes more uniform, and the difference between the peak and valley decreases.

In the process of tool dressing, the radial wear of tool makes the maximum height of tool contour decrease, which leads to the actual cutting position of tool moving backward and reduces the cutting load of tool front end. Meanwhile, the radial wear of the tool makes the tool smooth, the cutting load fluctuation caused by the contour height fluctuation is reduced, and the tool cutting load is more uniform. Therefore, with the tool dressing, the cutting force at the front end gradually decreases, and the peak value of the cutting force decreases, and the fluctuation of the cutting force is also smaller, which is conducive to improving the stability of the honing process.

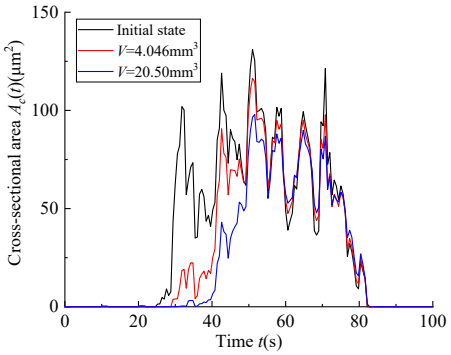

Fig. 9 Influence of tool contour on $A_c(t)$

4 Influence of cutting parameters on surface roughness

Surface roughness is one of the evaluation indexes of the surface integrity of parts, which has an important impact on the wear resistance, fatigue resistance of fuel nozzles. The surface roughness is one of the important factors that limit the improvement of machining efficiency. Therefore, the basis of realizing the optimization of single-pass honing process is to clarify the influence law of process parameters on surface roughness.

4.1 Influence of spindle speed on surface roughness

When feedrate per revolution is 10 μm/r and retracting speed is 50 μm/r, surface roughness under different spindle speed is shown in Fig. 10. The surface roughness is between R_a0.181μm and R_a0.189μm at different tool speeds, which has little change. Only changing the spindle speed, the cutting paths of the effective grains and $A_c(t)$ do not change, thus the surface roughness formed by cutting is basically unchanged. Therefore, it can be considered that the spindle speed has no effect on the surface roughness when the feedrate per revolution and tool retracting rate per revolution remain unchanged in the range of parameters used in the test. However, with the increase of spindle speed, the feedrate and withdrawal rate can be increased correspondingly on the premise that the surface roughness remains unchanged, so as to improve the machining efficiency. Therefore, the following tests will be carried out at the spindle speed of 5000 rpm.

4.2 Influence of feedrate on surface roughness

When spindle speed is 5000 rpm and retracting speed is 200 mm/min, the influence of feedrate on surface roughness is shown in Fig. 11. Surface roughness gradually increases with feedrate increasing. When feedrate increases from 20 mm/min to 100 mm/min, surface roughness increases from 0.1468 μm to 0.2048 μm. The machined surface morphology and contour height distribution

obtained at different feedrates are shown in Fig. 12. According to Fig. 7, the slower the feedrate is, the smaller the maximum $A_c(t)$ is, the shallower the surface scratch of the workpiece is. Furthermore, by comparing Fig. 12(a) and Fig. 12(b), when the feedrate is slow, the height difference between the wave peek and the wave valley is small, thus the lower surface roughness can be obtained. It can also be seen from Fig. 12(b) that a single grain continuously cuts the hole wall to produce equal interval cutting grooves. The interval of the deepest continuous groove is about 40 μm, which is the same as the retracting rate per revolution. Therefore, it can be concluded that when the feedrate is 100mm/min, the tool retracting not only remove the residual material on the workpiece surface, but also cut the deeper material, resulting in new and deeper cutting grooves.

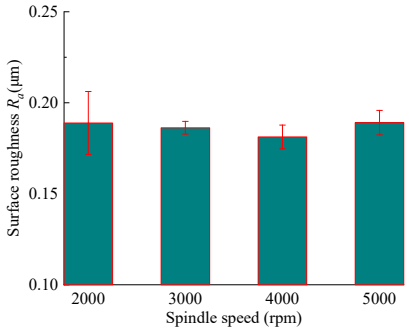

Fig. 10 Influence of spindle speed on roughness

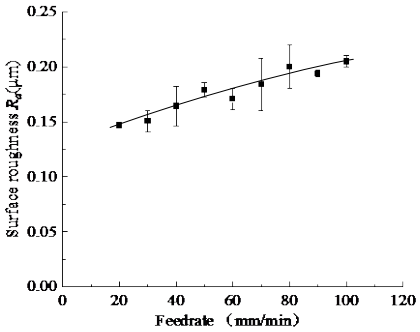

Fig. 11 Influence of feedrate on roughness

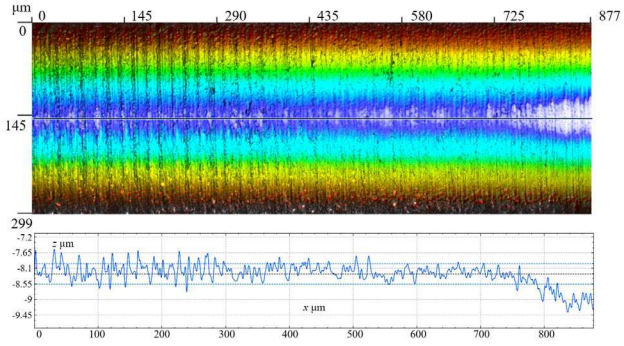

(a) Feedrate 20mm/min

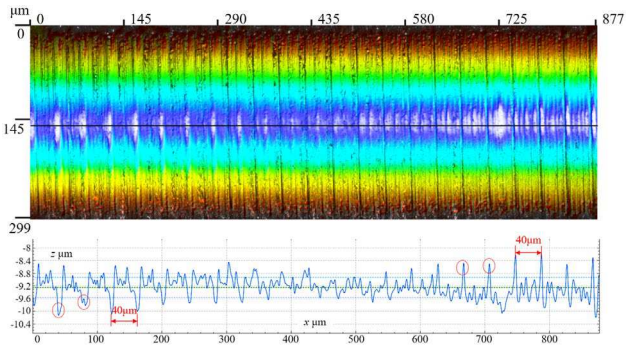

(b) Feedrate 100mm/min

Fig. 12 Surface roughness and height distribution of cross section on different feedrates

In single-pass honing process, the micro formation process of the surface morphology of the workpiece is shown in Fig. 13. In the tool feeding stage, due to cutting force, the workpiece surface will have a slight elastic deformation, resulting in the actual maximum cutting height y_{wv} of the workpiece surface is less than the maximum height y_{max} of the tool. In the tool retracting stage, the cutting allowance of the workpiece surface is small, and the cutting force is also small. Meanwhile, the elastic deformation of the workpiece is less than that of the feeding stage. Therefore, the grains will produce new cutting grooves in the elastic deformation zone of the feeding stage. When the tool feedrate is increased, the cutting force in the feeding stage increases gradually. The thickness of the elastic deformation zone generated in the feeding process gradually increases, which makes the cutting scratch generated on the workpiece surface in the tool retracting stage more obvious, as shown in Fig. 12(b).

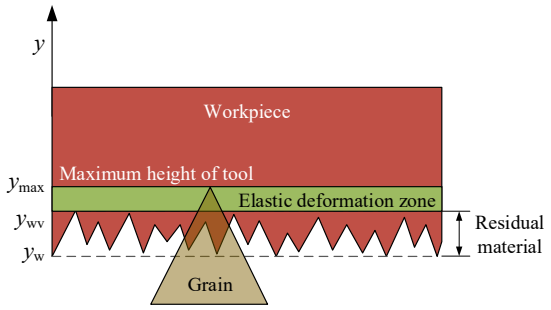

Fig. 13 Micro formation process of the surface morphology

4.3 Influence of retracting speed on surface roughness

From the above analysis, the residual material on the workpiece surface in the feed stage is removed, which can improve surface roughness. However, the new cutting grooves are created in the elastic deformation area, which can deteriorate surface roughness. In order to study the influence of tool retracting speed on surface roughness, the test was carried out under the conditions of tool speed 5000 rpm and feedrate 100 mm/min. the measured surface roughness is shown in Fig. 14. Reducing the tool retracting speed can effectively improve the machined surface roughness. When the retracting speed is reduced from 500 mm/min to 10 mm/min, the surface roughness decreases from 0.24 μm to 0.08 μm. According to Fig. 14, with the decrease of tool retracting speed, the effect of improving surface roughness becomes more and more prominent, which accelerates the reduction speed of surface roughness. When the retracting speed is 10mm/min, the machined surface morphology and profile height distribution are shown in Fig. 15, where the machined surface has no obvious scratches and leads to better surface quality.

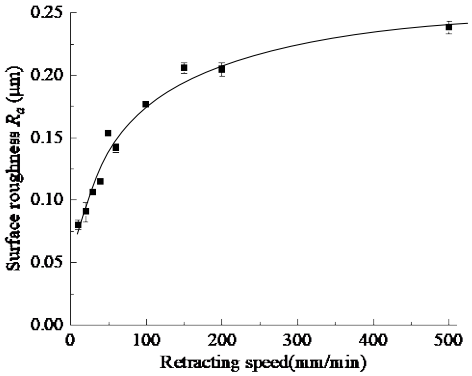

Fig. 14 Influence of withdrawal speed on surface roughness

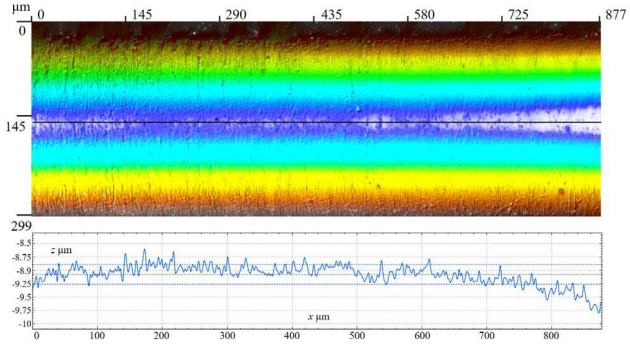

Fig. 15 Surface morphology and height distribution with retracting speed 10mm/min

5 Influence of cutting parameter on geometric accuracy

Bore diameter and shape accuracy are two important indexes to evaluate the geometric accuracy of a hole. The bore diameter of the inlet and outlet is taken as the evaluation index of bore diameter, and the absolute value of the difference between the inlet and outlet bore diameters is used as the evaluation index of shape accuracy.

5.1 Influence of spindle speed on geometric accuracy

Keeping the feedrate per revolution 110 μm/r and tool retracting rate per revolution 50 μm/r unchanged, the bore diameter and shape accuracy obtained at different spindle speeds are shown in Fig. 16. With spindle speed increasing, the inlet diameter remains unchanged, while the outlet diameter increases gradually. When the spindle speed increases from 2,000 rpm to 5,000 rpm, the outlet diameter increases from 0.7785 mm to 0.7806 mm, resulting in the increase of shape error from 0.6 μm to 1.9 μm.

In honing, the residual material and the elastic deformation under the action of cutting force lead to the bore diameter slightly smaller than the maximum diameter of the tool. When the tool parameters remain unchanged, the cutting force and residual height in the machining process will affect the bore diameter. When the feedrate per revolution is the same, the cutting force is similar, and the elastic deformation caused by the cutting force is also similar. In addition, with the same

feedrate per revolution, the roughness machined surface remains unchanged and the height of residual material remains unchanged only with the increase of spindle speed. Therefore, when the feedrate per revolution is the same, only increasing the spindle speed, the bore diameter obtained should remain unchanged, which is consistent with the inlet diameter.

However, with the tool feeding, the length extending out of the workpiece gradually increases. Under the influence of the uneven mass of the tool and the clamping position error of the initial hole, there is a certain eccentric mass between the tool and the rotary axis. When the tool rotates at high speed, under the action of centrifugal force, the part of the tool extending out of the workpiece will deform elastically. When the centrifugal force and the deformation resistance of the tool reach balance, it will reach a stable state, as shown in Fig. 17. The tool deformation will lead to the bore diameter increasing at the outlet and form a trumpet hole. With the increase of tool speed, the centrifugal force increases, the deformation of the tool end increases, and the outlet diameter and hole shape error also increase.

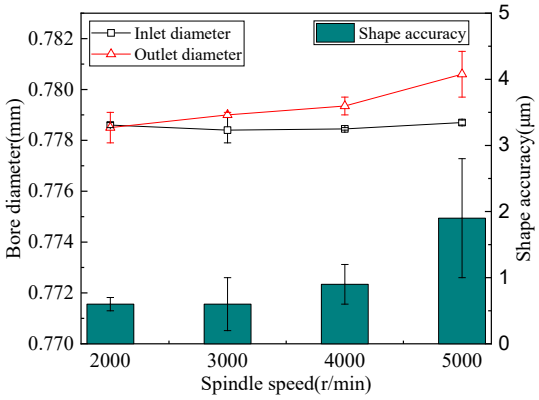

Fig. 16 Bore diameter and shape accuracy under different spindle speeds

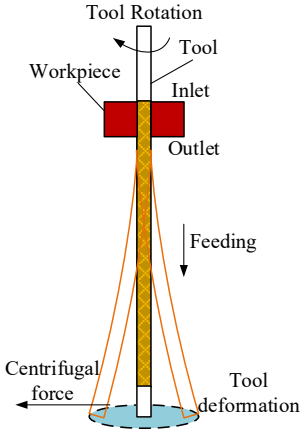

Fig. 17 Swing diagram of honing tool

5.2 Influence of feeedrate and retracting speed on geometric accuracy

When the spindle speed is 5000 rpm and the retracting speed is 200mm/min, the influence of feedrate on the bore diameter and shape accuracy is shown in Fig. 18. When the spindle speed is 5000 rpm and the feedrate is 100 mm/min, the influence of retracting speed on the bore diameter and shape accuracy is shown in Fig. 19. Under the above processing parameters, the outlet diameter is always larger than the inlet diameter. With the increase of feedrate or retracting speed, the outlet diameter decreases significantly, while the inlet diameter only slightly decreases, and the shape accuracy of the hole is also improved. When the retracting speed is further increased, the bore diameter and shape error are basically unchanged. Compared with Fig. 18 and Fig. 19, increasing the tool retracting speed can reduce the outlet diameter and improve the shape error significantly.

The elastic deformation of the tool under the action of centrifugal force increases the outlet diameter, resulting in the outlet diameter larger than the inlet diameter. However, the cutting effect of tool end deformation on the hole outlet is similar to constant force cutting, and material removal volume is determined by both pressure and cutting time [16]. When the speed of the tool remains unchanged, it can be approximately considered that the pressure of the deformed tool on the outlet hole wall remains unchanged. With the increase of feedrate or retracting speed, the total cutting time is shortened, and the material removal volume at the outlet is reduced, which leads to the decrease of the outlet diameter and shape error. In the feeding stage, most of the machining allowance is removed, and the bore diameter increases rapidly. The shape error in the feeding stage can be corrected by the subsequent material removal. However, the residual material is removed by tool retracting sightly, and the shape error is completely retained in the final part. Therefore, compared with the feedrate, the tool retracting speed has a greater impact on the final bore diameter and shape error.

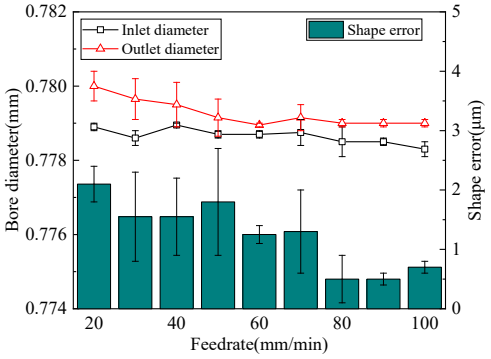

Fig. 18 Influence of feedrate on bore diameter and shape accuracy

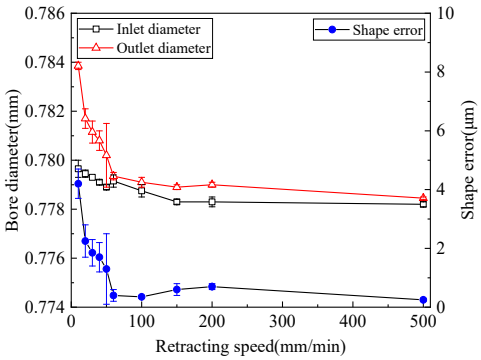

Fig. 19 Influence of retracting speed on bore diameter and shape accuracy

6 Optimization of honing parameters

When single-pass honing tool is applied to fuel nozzle machining, honing parameters should be optimized according to the above discussion, to achieve the highest processing efficiency under the premise of meeting machining accuracy. Therefore, the shape accuracy and surface roughness are taken as the technical indexes to optimize the single-pass honing parameters.

Under the condition that the feedrate per revolution and tool retracting speed per revolution remain unchanged, increasing the spindle speed will increase the feedrate and retracting speed, thus improving the honing efficiency. At the same time, surface roughness remains basically unchanged, but the deformation of the tool end will reduce the shape accuracy of the hole, and even cause tool damage. Considering the machining efficiency, shape accuracy and machining stability, it is safe to set 5000 rpm as the spindle speed.

According to the above analysis, the feedrate and retracting speed will affect the shape accuracy. Fig. 20 shows the shape error of the hole obtained when the feedrate and retracting speed change together at the tool speed of 5000 rpm. When the feedrate and retracting speed are both not less than 20 mm/min, the shape error is less than 3 μm. Therefore, the feedrate and retracting speed used in single-pass honing are not smaller than 20 mm/min, which can meet the design requirements of shape error of 4 μm. Finally, taking the surface roughness as the index, the feedrate and tool retracting speed will be further optimized within parameter range.

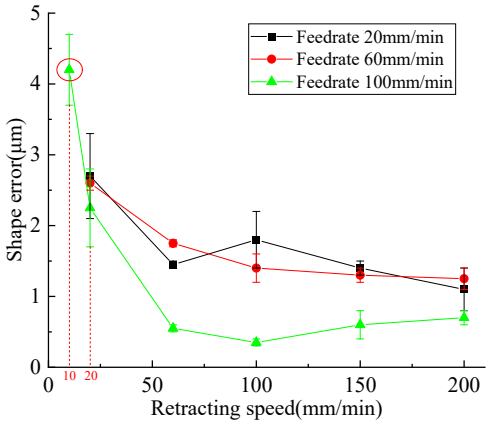

Fig. 20 Shape accuracy under different feedrate and retracting speed

The machined surface morphology obtained by single-pass honing is formed by the combined action of feeding and retracting, and the elastic deformation thickness and residual material produced in the feeding process will affect the micro cutting state of the retracting process. In order to study the interaction between feedrate and retracting speed and the influence on surface roughness, the full factor test of feedrate and retracting speed was carried out with spindle speed of 5000 rpm. Finally, surface roughness is shown in Fig. 21. The higher the retracting speed, the greater the influence of feedrate on surface roughness. When smaller retracting speed is taken, most of the surface topography formed in the feeding process will be cut off in the retracting process, so the influence of the feedrate on the final surface roughness is small. When larger retracting speed is taken, the tool retracing process has little effect on the surface topography of the workpiece, and the surface topography is mainly formed during the feeding process, which shows that the feedrate has a greater impact on the surface roughness. When the tool feedrate and retracting speed are small, the surface roughness obtained by single-pass honing is also small. Therefore, when the required surface roughness is 0.1 μm, the tool feedrate can be appropriately increased and the lower retracting speed can be used to obtain higher machining efficiency. When the required surface roughness is 0.2 μm, the tool retracting speed can be appropriately increased to improve the machining efficiency.

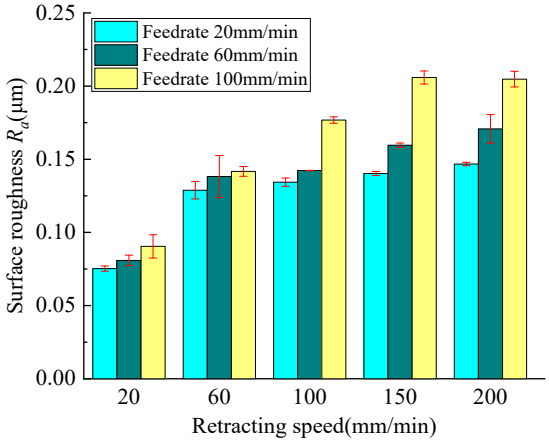

Fig. 21 Surface roughness under different feedrate and retracting speed

In order to realize the precise optimization of process parameters, it is necessary to establish the mathematical model of the influence of feedrate and retracting speed on surface roughness. The empirical formula of roughness can be expressed as [15]

$$R_a = C_0 F_1^{C_1} F_2^{C_2} \tag{13}$$

Where R_a is surface roughness, F_1, F_2 are feedrate and retracting speed respectively, C_1, C_2 are the influence indexes of feedrate and retracting speed respectively, and C_0 is a coefficient related to conditions other than feedrate and retracting speed. The logarithm of Eq. (13) is obtained

$$\ln R_a = \ln C_0 + C_1 \ln F_1 + C_2 \ln F_2 \tag{14}$$

The linear least square method is used to fit the parameters of Eq. (14), and the parameters, namely, C_0 = 0.01852, C_1 = 0.1466 and C_2 = 0.3247, can be obtained. Contour map of roughness with respect to feedrate and retracting speed is shown in Fig. 22.

The schematic diagram of feeding stroke and retracting stroke is shown in Fig. 23. When the minimum initial bore diameter is 0.75mm, the tool will not contact the workpiece until it is fed to point W, and rapid feed is used before point W. Because the rapid feedrate is far greater than the feedrate in single-pass honing, the fast feed time can be ignored. When the tool is fed to point W', the finishing part of the tool has passed through the workpiece completely and the tool starts retracting. Since the residual height of the workpiece surface is very small, the tool has been completely separated from the workpiece when the tool is retracted to the point W''. After that, the tool continues retracing with fast retracting speed, and the surface roughness will not be affected. Because the rapid retracting speed is far greater than the retracting speed in single-pass honing, the fast retracting time can be ignored.

$$T_m = \frac{50}{F_1} + \frac{30}{F_2}, \quad 20 \le F_1 \le 100,\ F_2 \ge 20 \tag{15}$$

In order to avoid excessive cutting force in the feeding process, which may cause machining

instability or even damage the tool, the maximum value of feedrate F_1 is set as 100 mm/min. the process parameters of single-pass honing meet

$$\begin{cases} 20 \le F_1 \le 100 \\ F_2 \ge 20 \\ C_0 F_1^{C_1} F_2^{C_2} \le R_{aD} \end{cases} \tag{16}$$

Where R_{aD} is the design value of nozzle surface roughness. Matlab is used to solve the nonlinear programming problem to obtain the optimal feedrate and retracting speed.

When the design requirement of fuel nozzle surface roughness is 0.1 μm, the optimal process parameters are spindle speed 5000 rpm, feedrate 100 mm/min, retracting speed 23.85mm/min, and the required processing time is 1.76 min. When the design requirement of fuel nozzle surface roughness is 0.2 μm, the optimal process parameters are spindle speed 5000 rpm, feedrate 100 mm/min, retracting speed 190 mm/min, and the required processing time is 0.66 min.

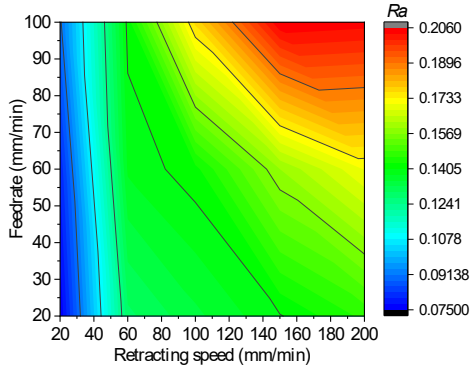

Fig. 22 Contour map of Ra

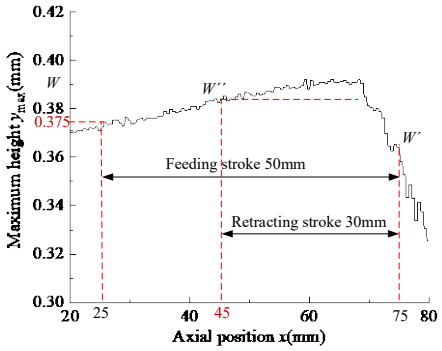

Fig. 23 Schematic diagram of feeding stroke and retracting stroke

7 Conclusion

Single-pass honing test was carried out by flexible honing tool. The process characteristics are explored, which are cutting force, surface quality and geometric accuracy, and the process parameters are optimized according to the design requirements. The main conclusions are as follows:

(1) The relationship model between cutting force and undeformed chip cross-sectional area $A_c(t)$ is established. The cutting force can be reduced by reducing the feedrate per revolution or the removal allowance.

(2) The surface roughness obtained under different process parameters shows that the spindle speed has no effect on the surface roughness when the feedrate per revolution remain unchanged. The surface roughness will increase with the increase of feedrate or tool retracting speed.

(3) The end of honing tool will deform due to centrifugal force, which will increase the outlet

bore diameter and shape error. When the feedrate per revolution remains unchanged, the outlet bore diameter and shape error will increase with spindle speed increasing. The outlet bore diameter and shape error will decreasing with feedrate and retracting increasing. When the feedrate and retracting speed are not less than 20 mm/min, the shape error is less than 3 μm.

(4) According to the requirements of nozzle honing, the process parameters are optimized within the allowable parameters range. When the surface roughness is 0.1 μm, the optimal process parameters are spindle speed 5000 rpm, feedrate 100 mm/min, retracting speed 23.85 mm/min, and the required processing time is 1.76min. When the surface roughness is 0.2μm, the optimal process parameters are spindle speed 5000 rpm, feedrate 100 mm/min, retracting speed 190 mm/min, and the required processing time is 0.66 min.

Ethical Approval

The article follows the guidelines of the Committee on Publication Ethics (COPE) and involves no studies on human or animal subjects.

Consent to Participate

Not applicable.

Consent to Publish

Not applicable.

Authors Contributions

Changyong Yang conceived the analysis and wrote the manuscript. Hao Su and Shaowu Gao performed the experiment and collected the data. Yucan Fu provided supervision on experiment. Wenfeng Ding and Jiuhua Xu revised the manuscript.

Funding

This work was funded by the National Natural Science Foundation of China (No. 52075252).

Competing Interests

The authors declare that they have no competing interests.

Availability of data and materials

All data generated or analyzed during this study are included in the present article.

References

[1] Liu YZ, Sun XX, Sethi V, Nalianda D, Li YG, Wang L. Review of modern low emissions combustion technologies for aero gas turbine engines. Progress Aerospace Science, 2017. 94:12-45.

[2] Tamaki N, Nishikawa K. Design of high-dispersion atomization nozzle for direct injection Diesel engine (Effects of shapes and measurement of nozzle holes of injection nozzle on spray and flow characteristics). Transactions of the Japan Society of Mechanical Engineers, 2015. 81(825):14-00228.

[3] Custer JR, Rizk NK. Influence of design concept and liquid properties on fuel injector performance. Journal of Propulsion & Power, 2011. 4(4):378-384.

[4] Gouskov AM, Voronov SA, Butcher EA, Sinha SC. Non-conservative oscillations of a tool for deep hole honing. Communication in Nonlinear Science & Numerical Simulation, 2006. 11(6):685-708.
[5] Moos U, Bähre D. Analysis of Process Forces for the Precision Honing of Small Bores. Procedia CIRP, 2015. 31:387-392.
[6] Klocke F, Kuchle A. Manufacturing processes 2: grinding, honing, lapping, 2009.
[7] Yousfi M, Demirci I, Mezghani S, EI Mansori M. Smoothness and plateauness contributions to the running-in friction and wear of stratified helical slide and plateau honed cylinder liners. Wear, 2015. 332-333:1238-1247.
[8] Yousfi M, Mezghani S, Demirci I, EI Mansori M. Mutual effect of groove size and anisotropy of cylinder liner honed textures on engine performances. Advanced Materials Research, 2014. 966-967:175-183.
[9] Arunachalam S, Gunasekaran A, O'Sullivan JM. Analysing the process behaviour of abrasive reaming using an experimental approach. International Journal of Machine Tools & Manufacture, 1999. 39(8): 1311-1325.
[10] Yang XR, Zhu YW, Qi X, Xu ZX. Optimization of the reaming honing process of valve sleeve based on orthogonal test. Diamond & Abrasive Engineering, 2013. 33:26-30. (In Chinese)
[11] Kholmogortsev YP. Optimizing the diamond reaming of precision holes. Russian Engineering Research, 2009. 29(4): 375-382.
[12] Yang CY, Su H, Gao SW, Ai QF, Xu JH. Characterization and life prediction of single-pass honing tool for fuel injection nozzle. Chinese Journal of Aeronautics, 2020.
[13] Gao SW, Yang CY, Xu JH, Fu YC, Su H, Ding WF. Optimization for internal traverse grinding of valves based on wheel deflection. International Journal of Advanced Manufacturing Technology, 2017. 92(1-4):1105-1112.
[14] Cao JG, Wu YB, Li JY, Zhang QJ. A grinding force model for ultrasonic assisted internal grinding (UAIG) of SiC ceramics. International Journal of Advanced Manufacturing Technology, 2015. 81(5-8): 875-885.
[15] Ren JX, Hua DA, Zhou WY. Grinding Theory. Electronic Industry Press, 2011. (In Chinese)
[16] Gao SW, Yang CY, Xu JH, Su H, Fu YC. Modelling and simulation of bore diameter evolution in finish honing. Procedia Manufacturing, 2018. 26: 462-468.

Figures

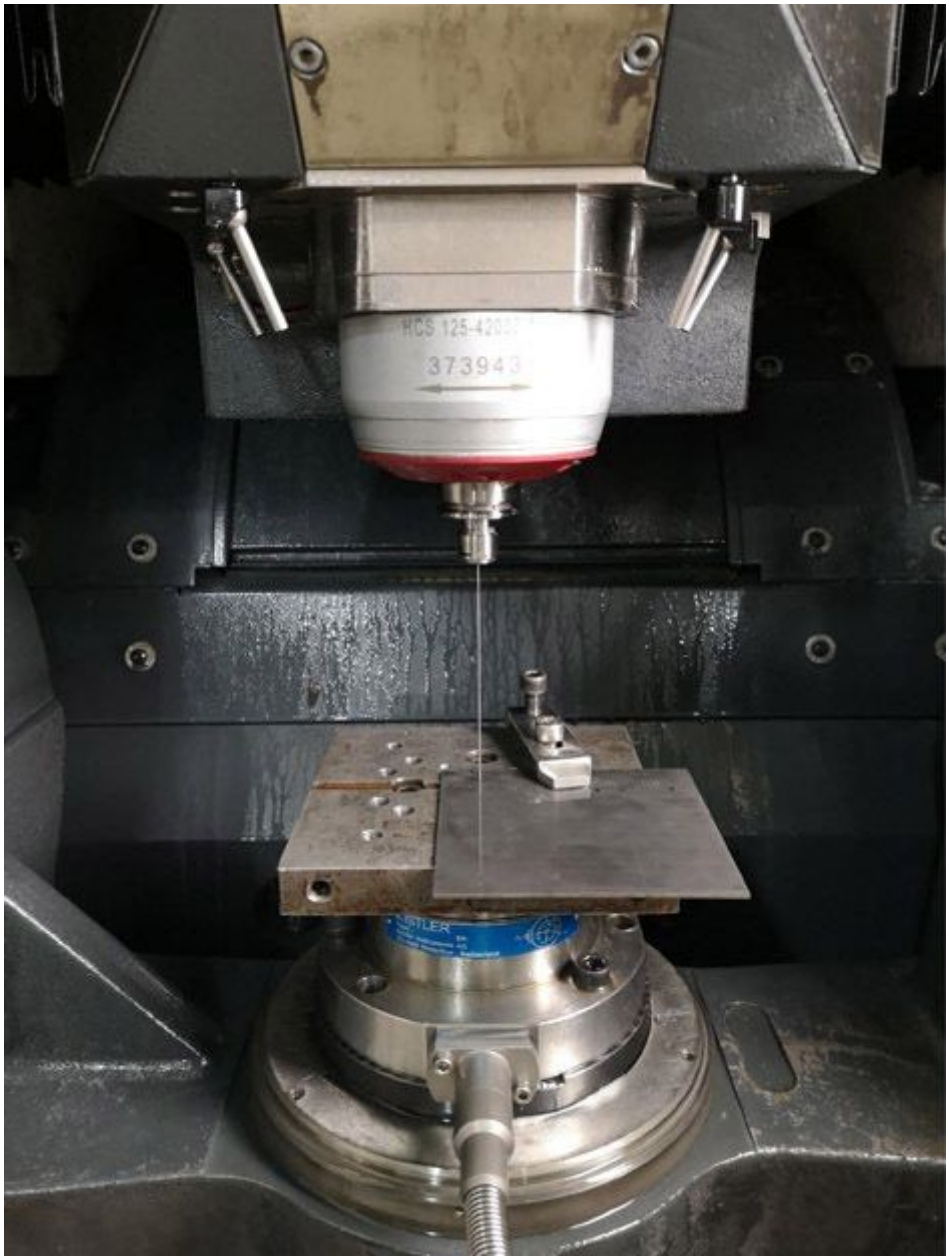

Figure 1

Single-pass honing platform

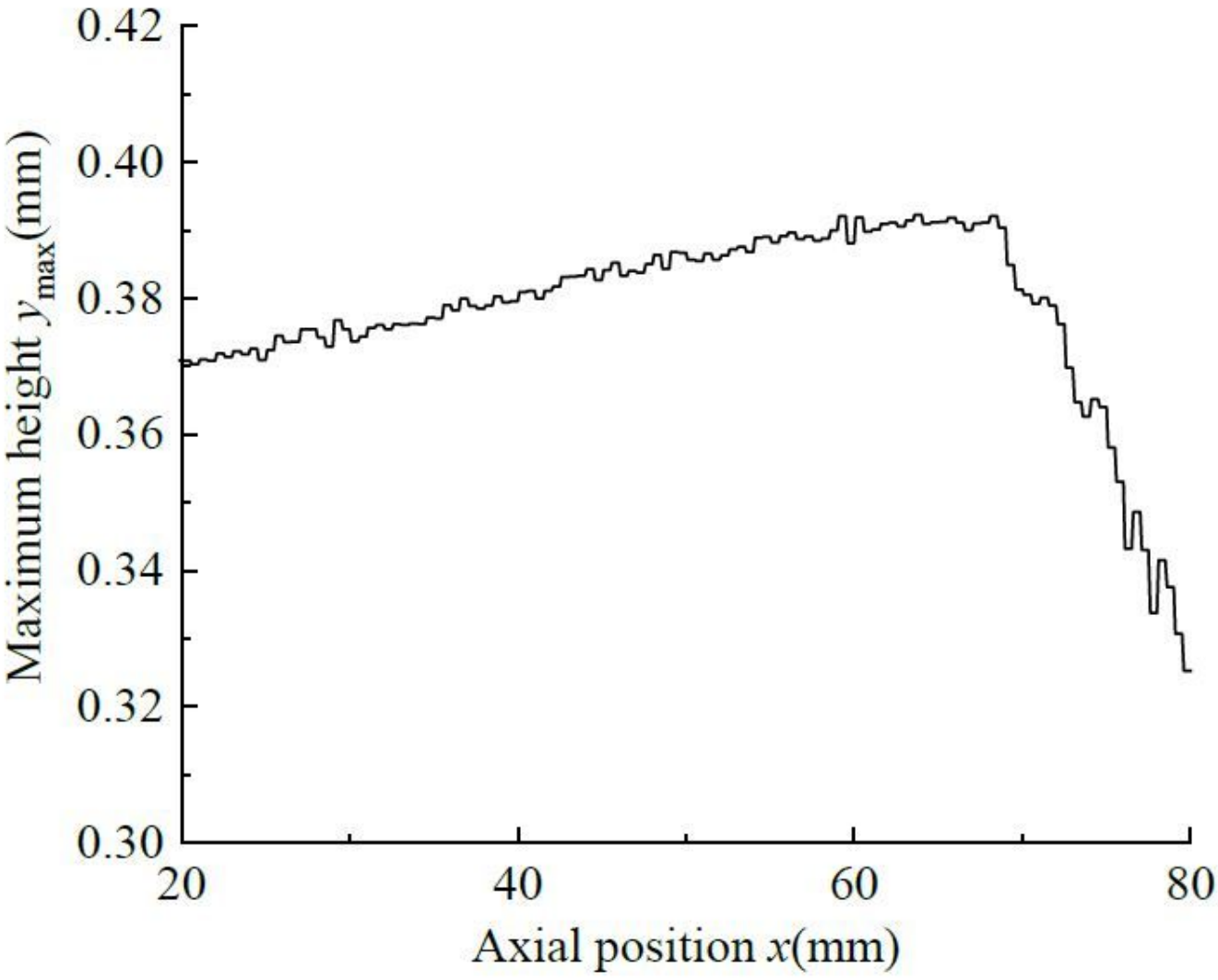

Figure 2

Maximum contour distribution of tool

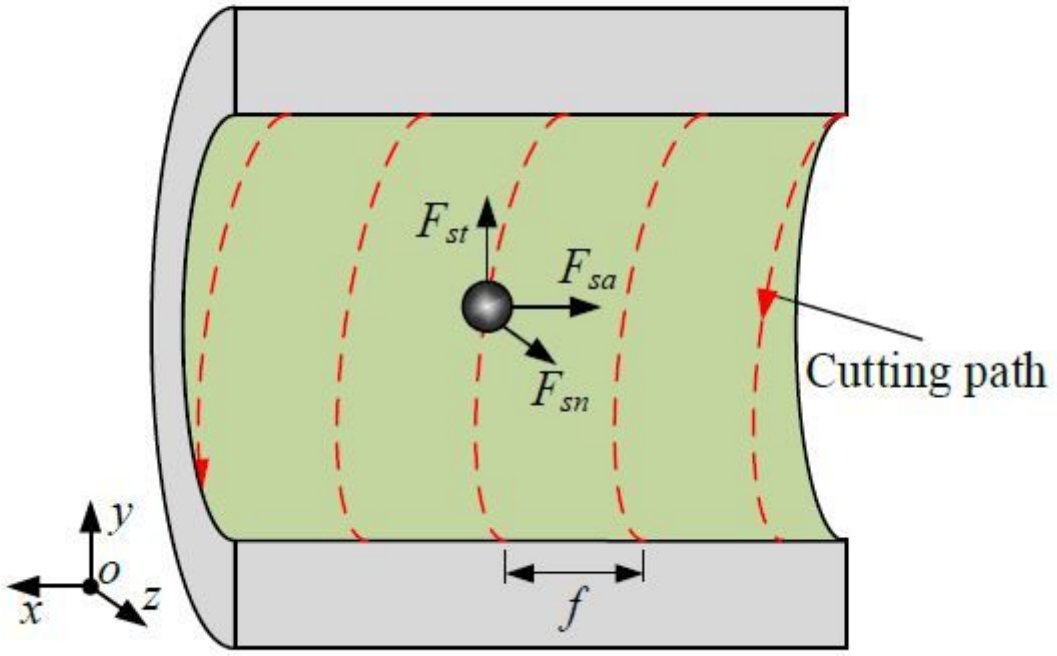

Figure 3

The force diagram of single grain

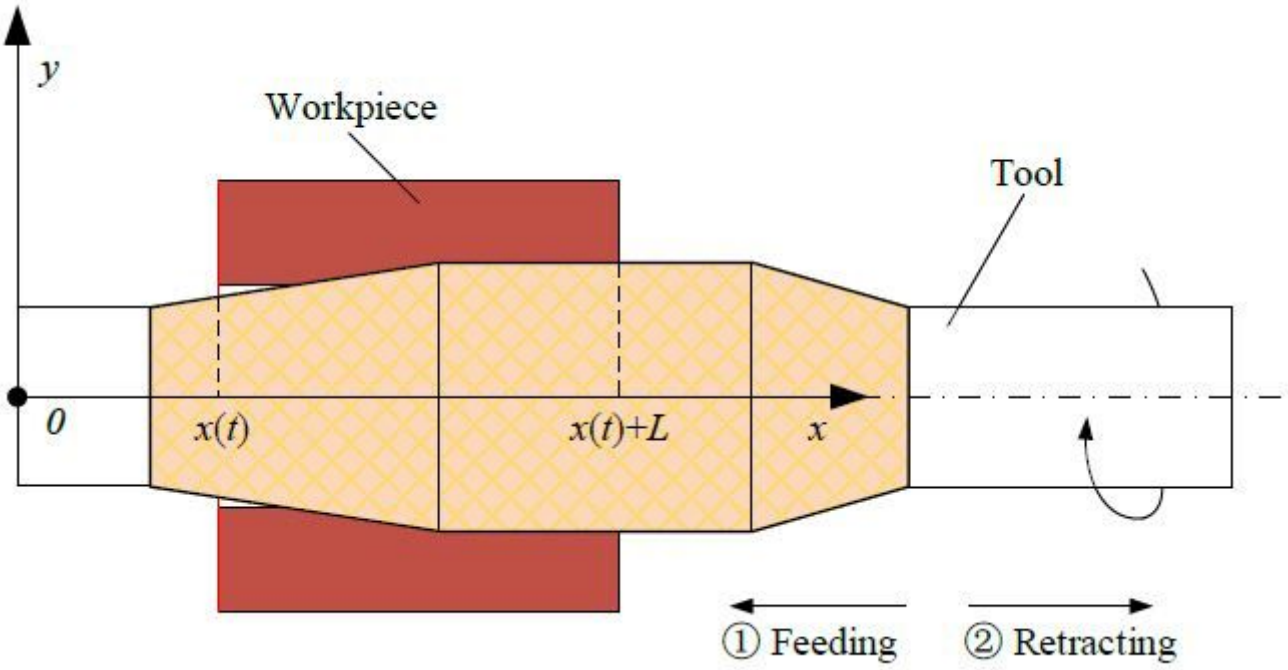

Figure 4

The relative position of tool and workpiece

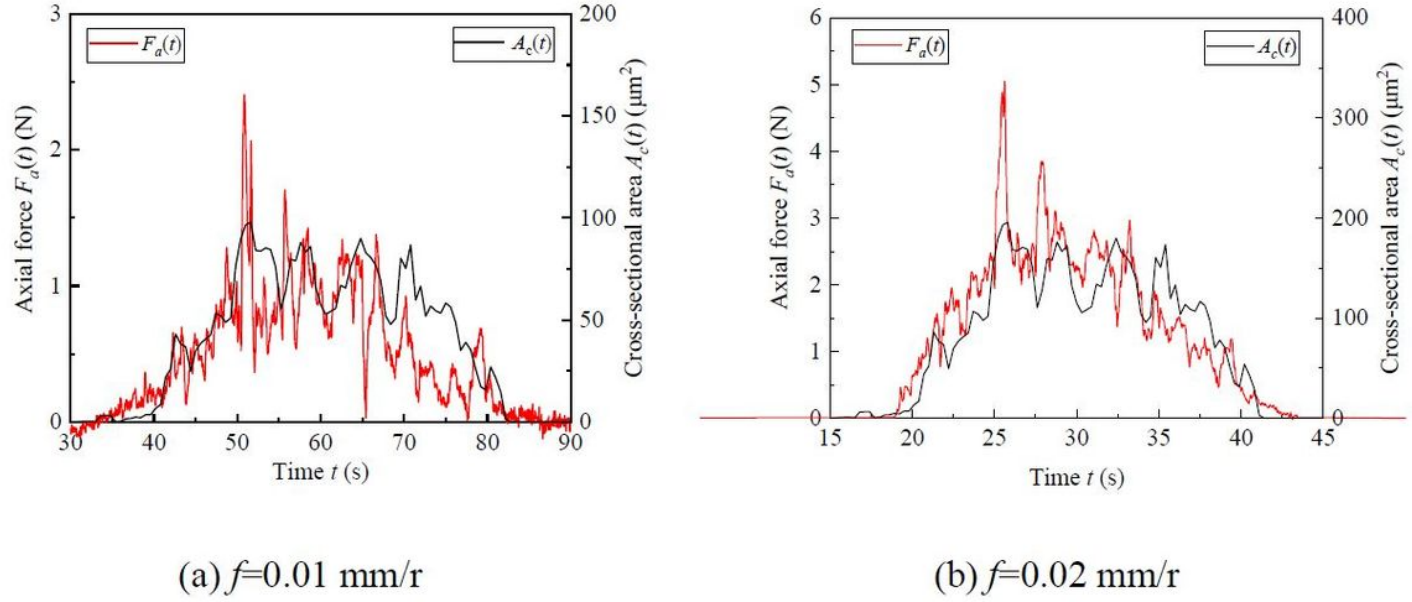

Figure 5

Measured Fa(t) and calculated Ac(t) under different f

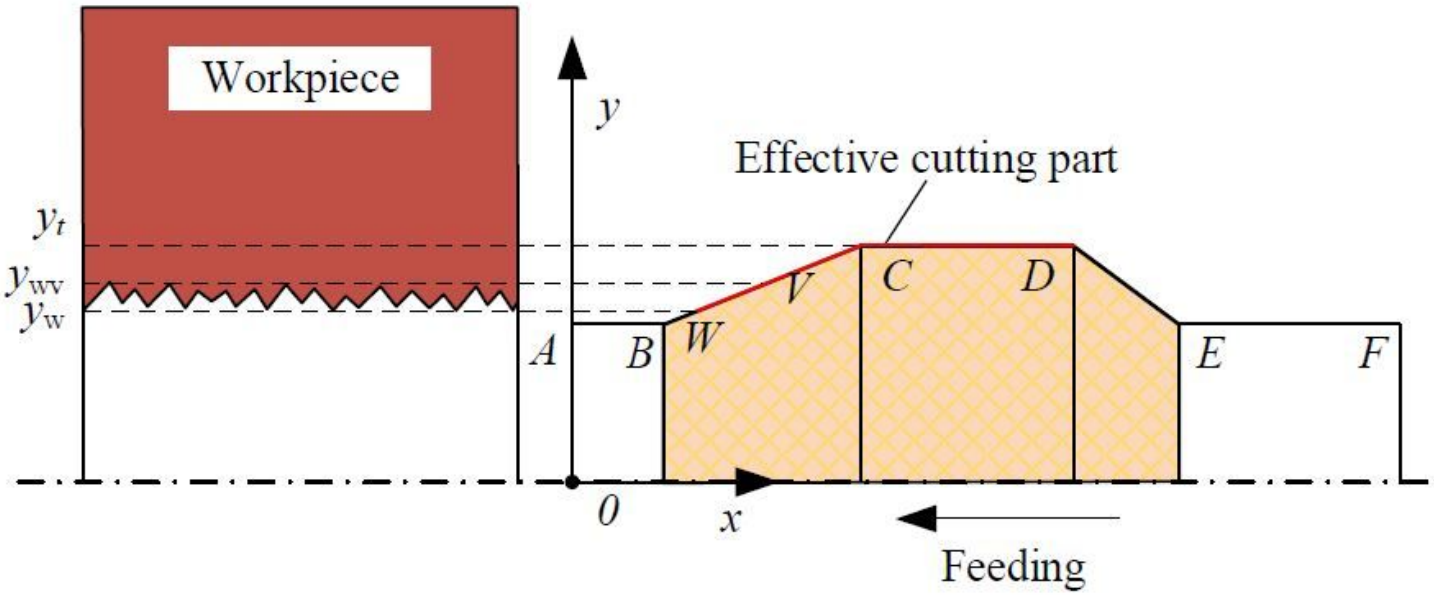

Figure 6

Contact diagram of micro contour between tool and workpiece

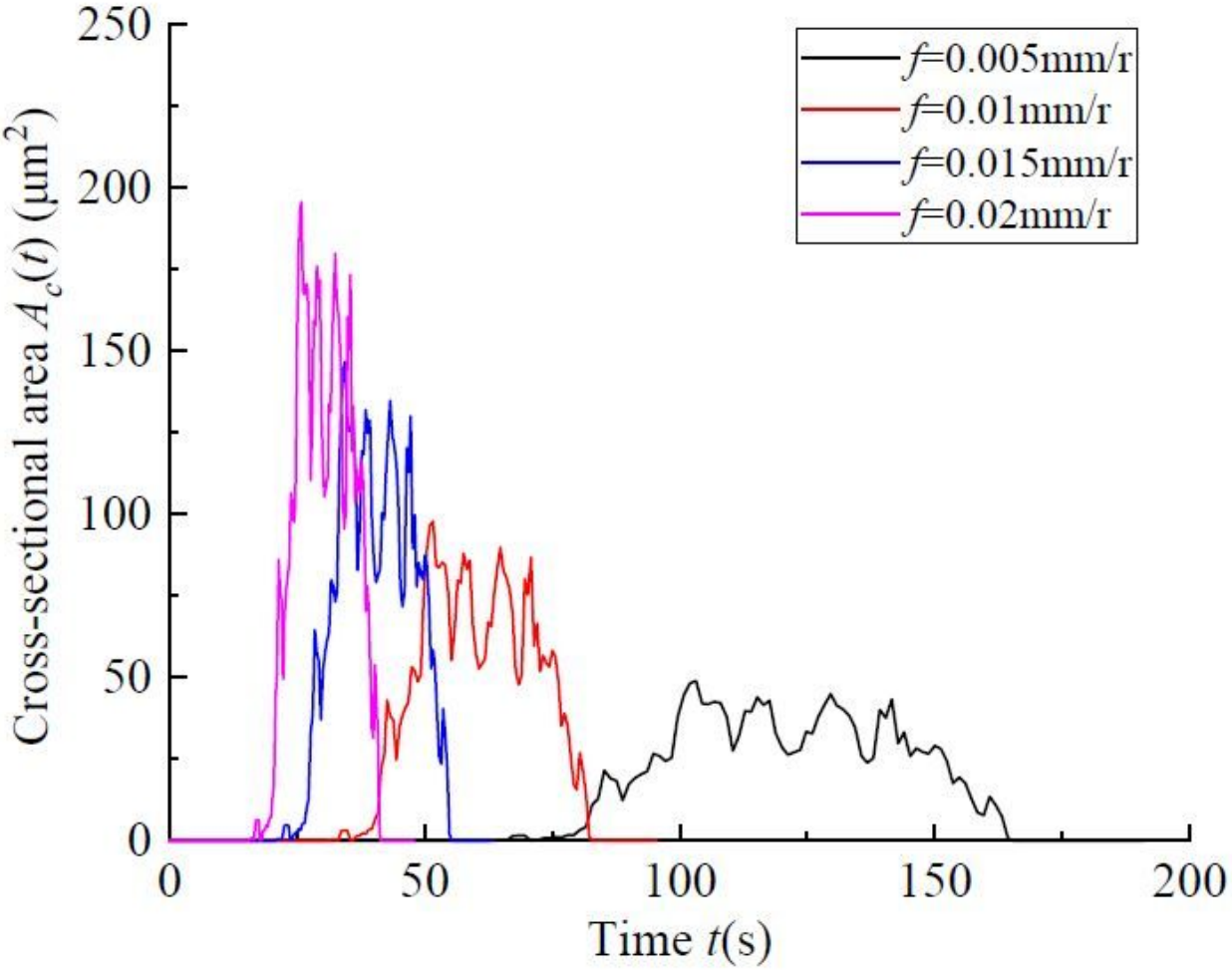

Figure 7

Influence of f on Ac(t)

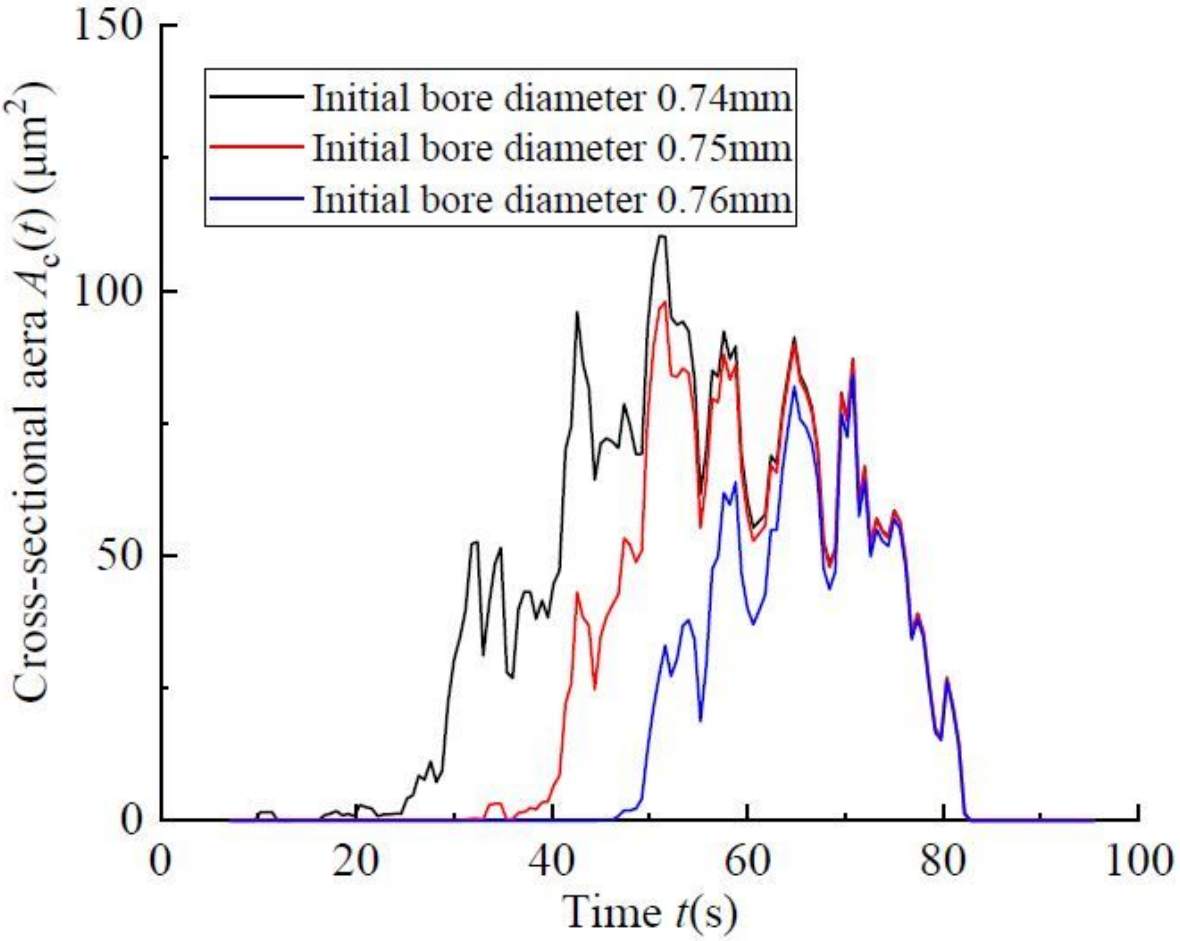

Figure 8

Influence of initial bore diameter on Ac(t)

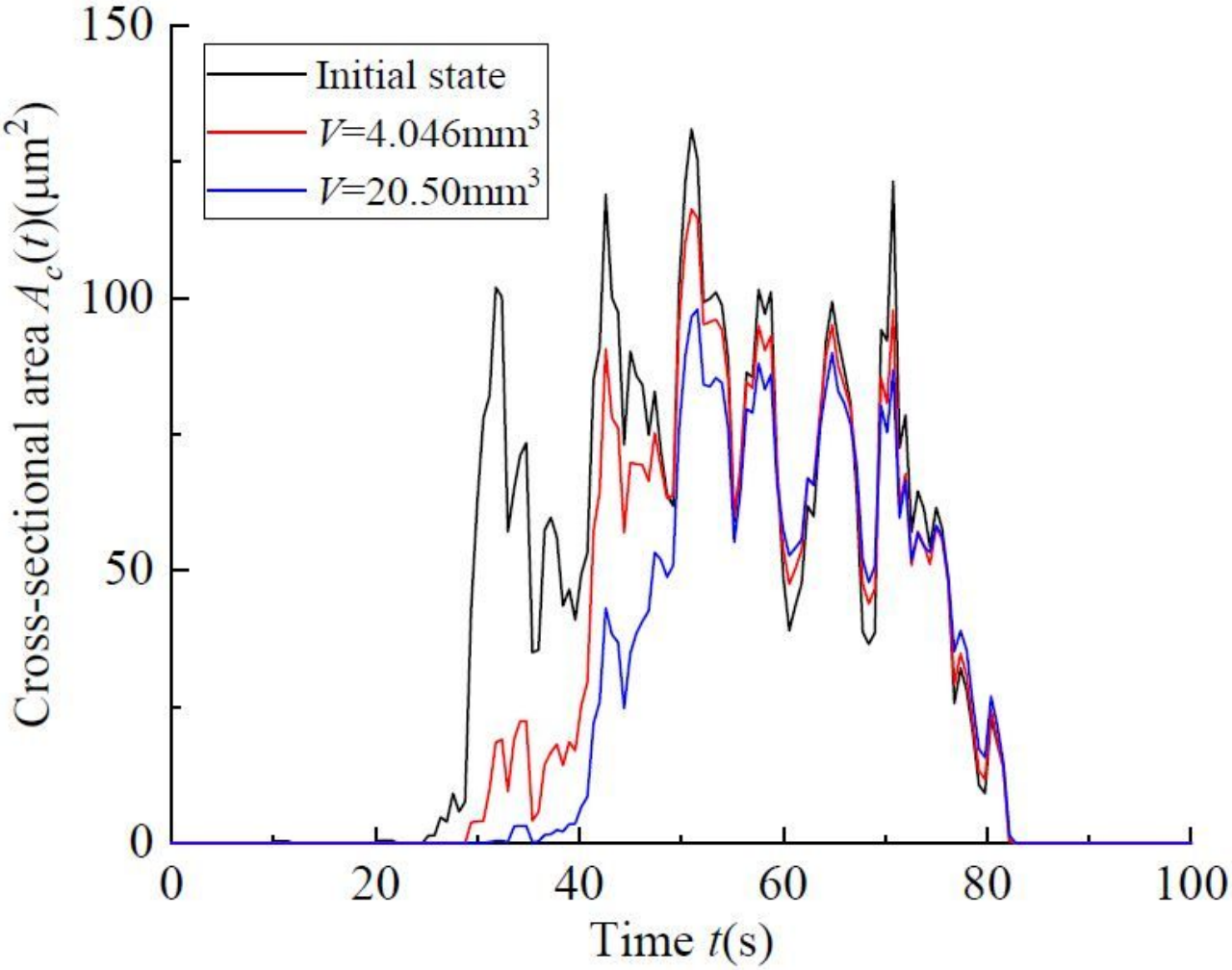

Figure 9

Influence of tool contour on Ac(t)

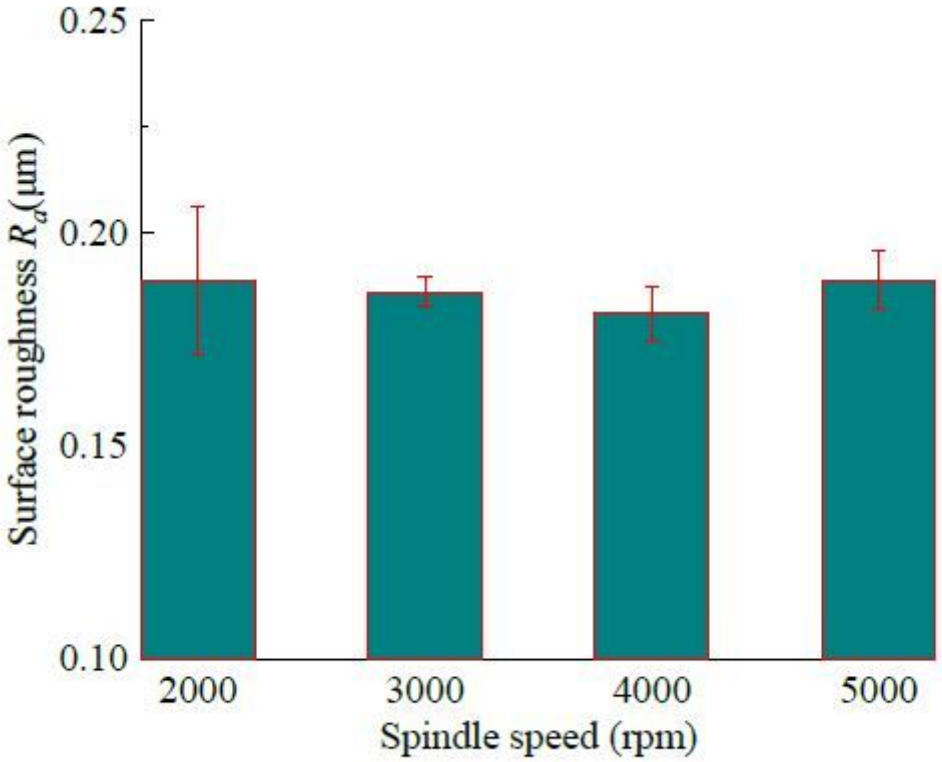

Figure 10

Influence of spindle speed on roughness

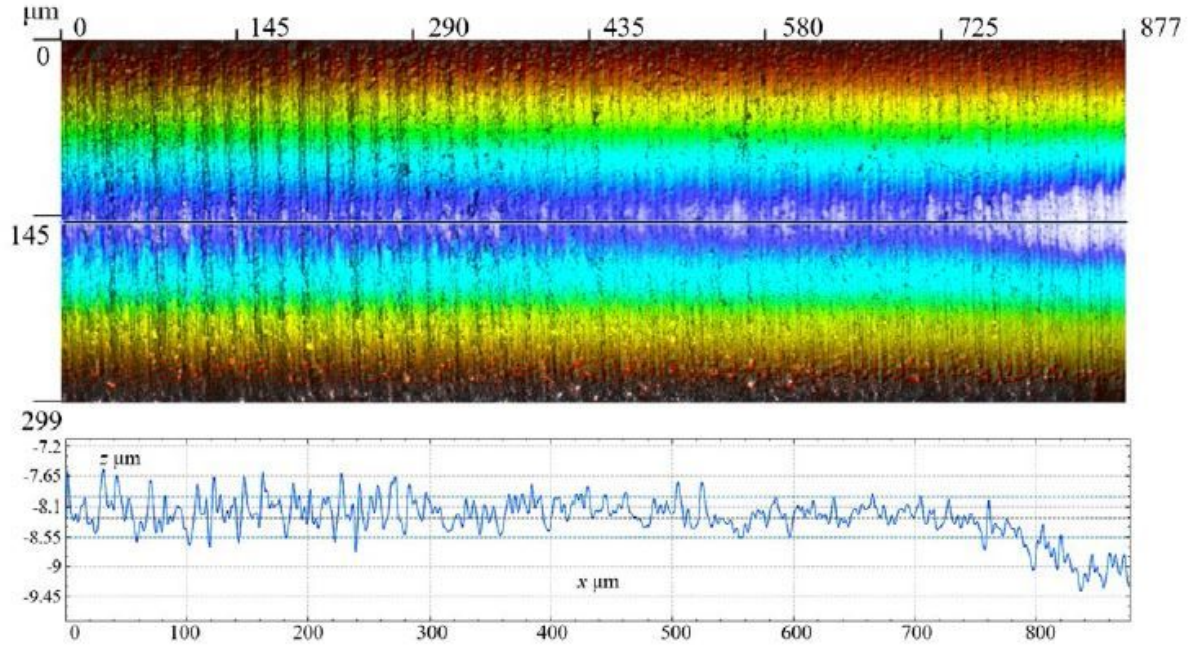

(a) Feedrate 20mm/min

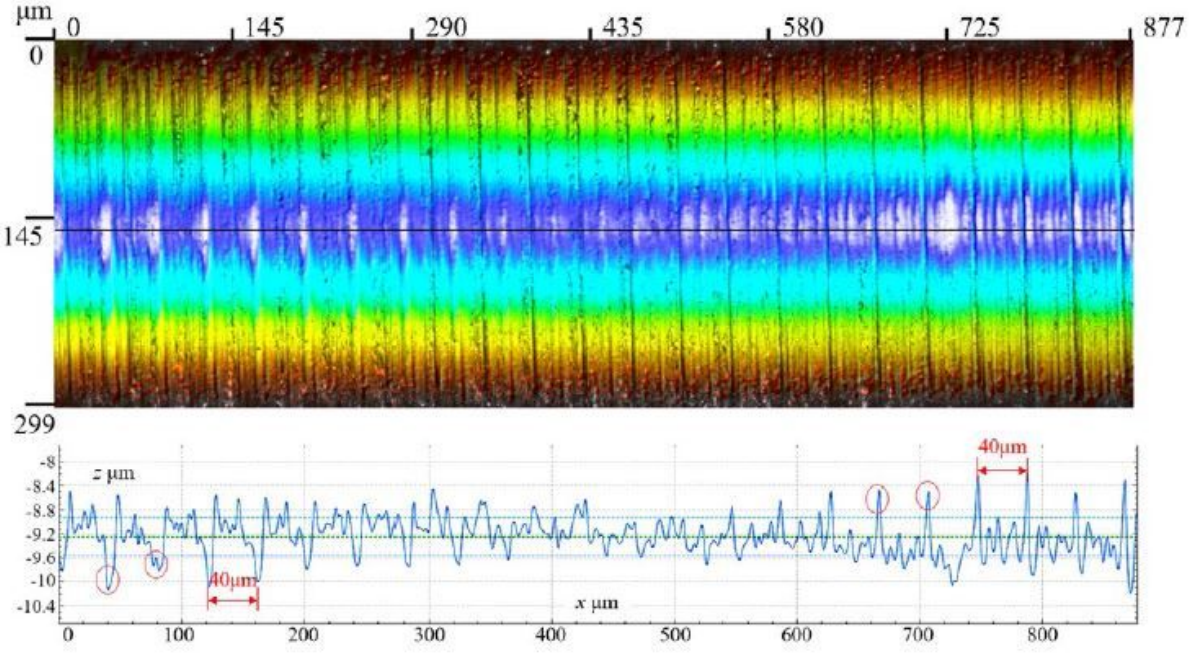

(b) Feedrate 100mm/min

Figure 12

Surface roughness and height distribution of cross section on different feedrates

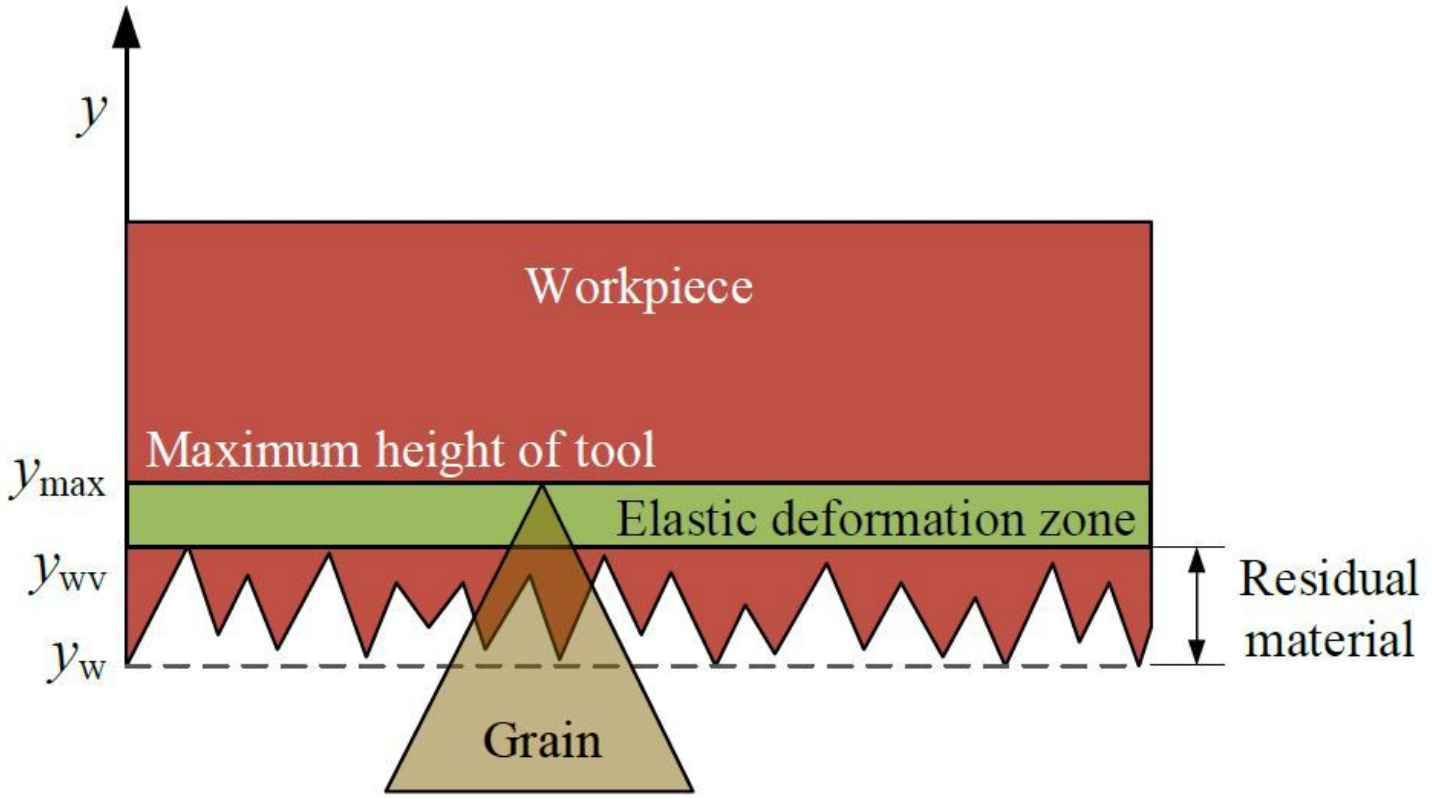

Figure 13

Micro formation process of the surface morphology

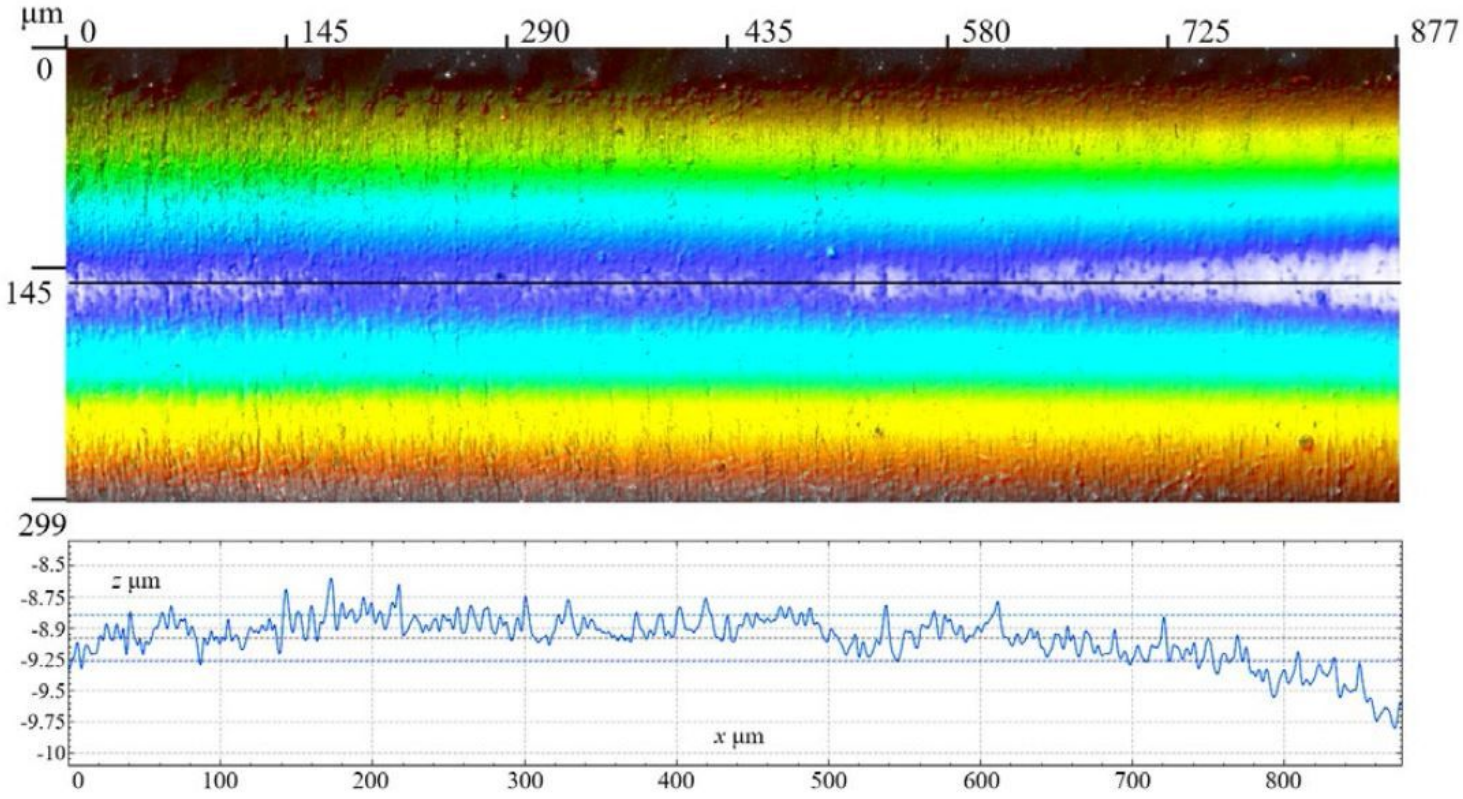

Figure 15

Surface morphology and height distribution with retracting speed 10mm/min

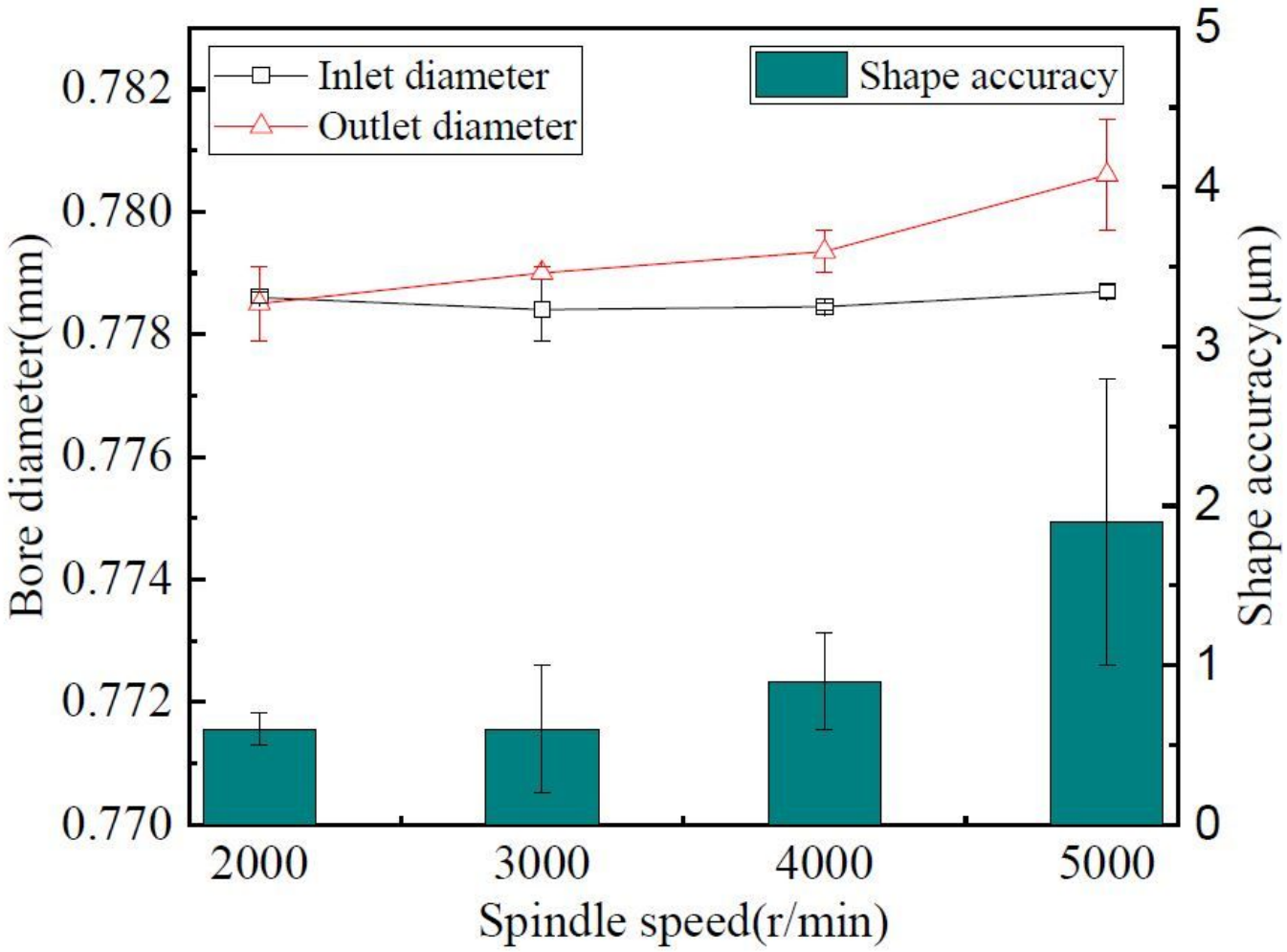

Figure 16

Bore diameter and shape accuracy under different spindle speeds

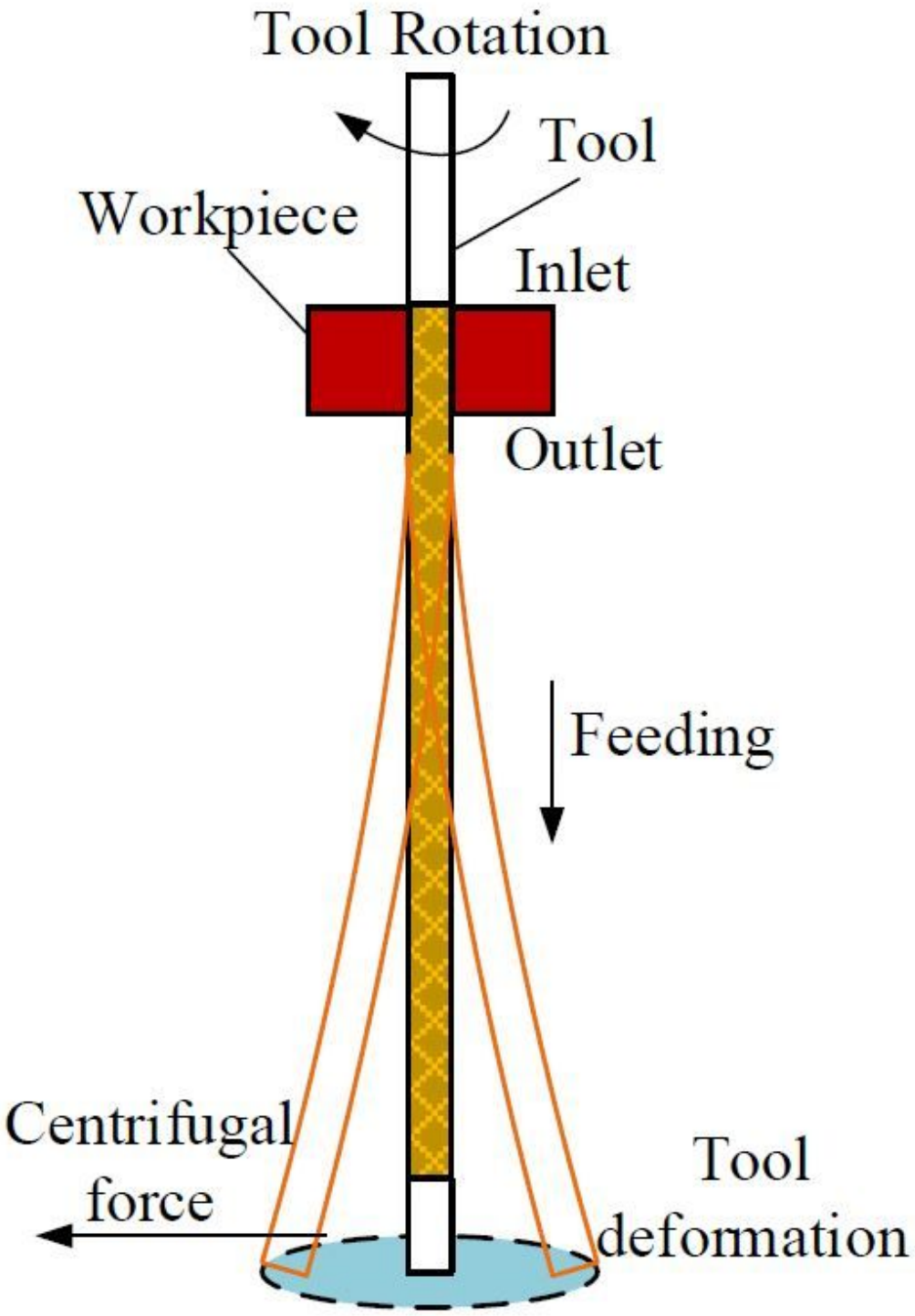

Figure 17

Swing diagram of honing tool

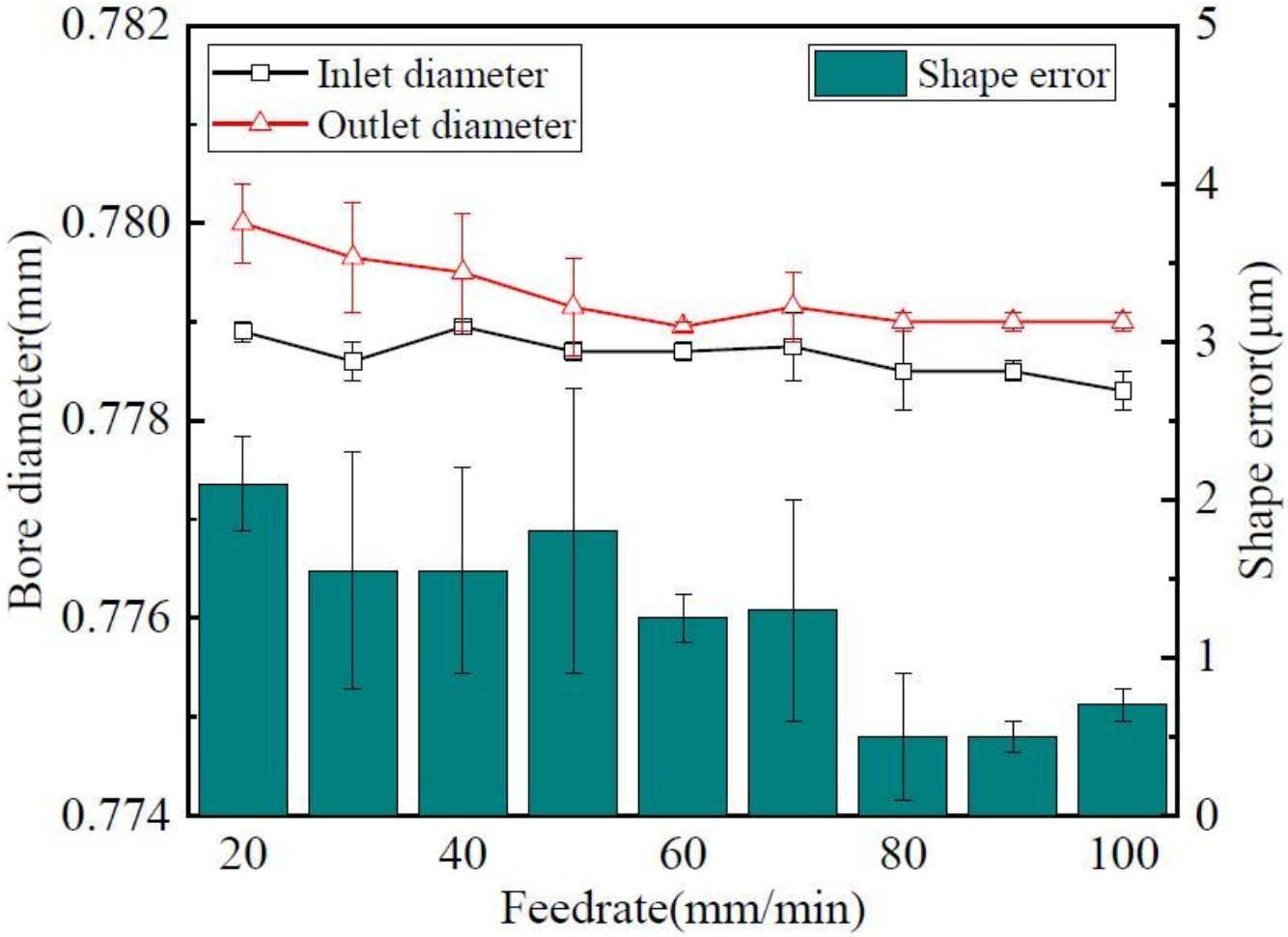

Figure 18

Influence of feedrate on bore diameter and shape accuracy

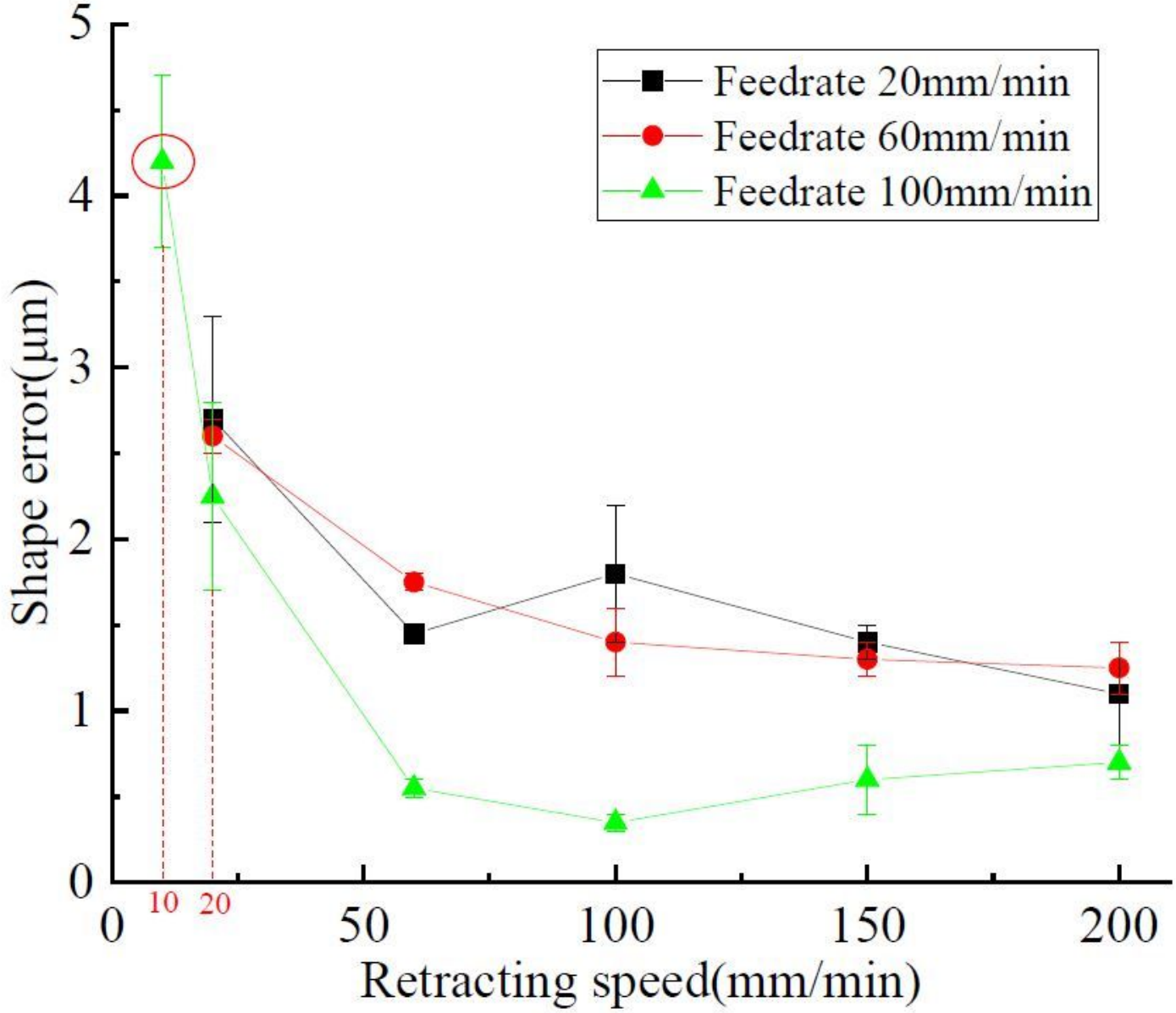

Figure 20

Shape accuracy under different feedrate and retracting speed

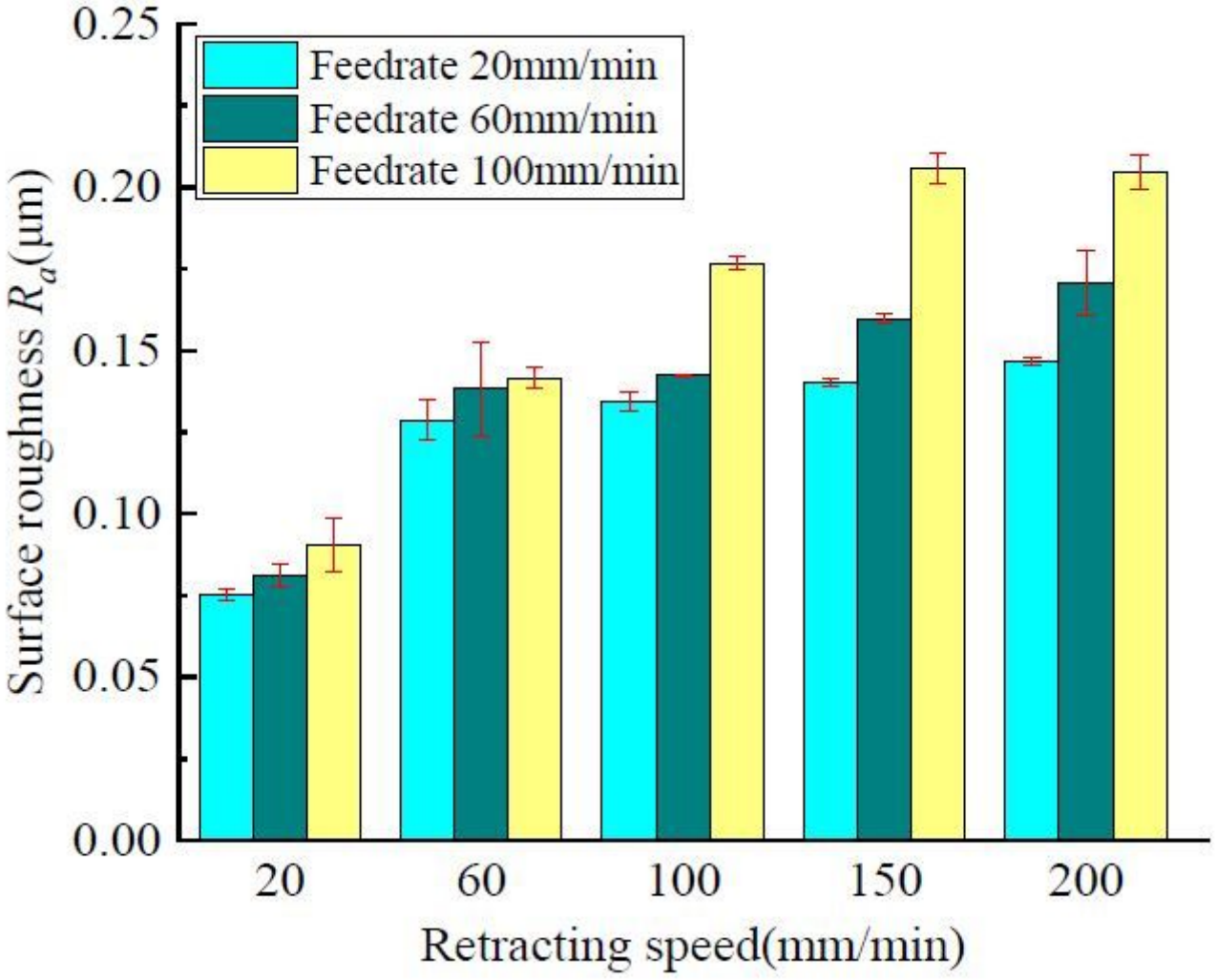

Figure 21

Surface roughness under different feedrate and retracting speed

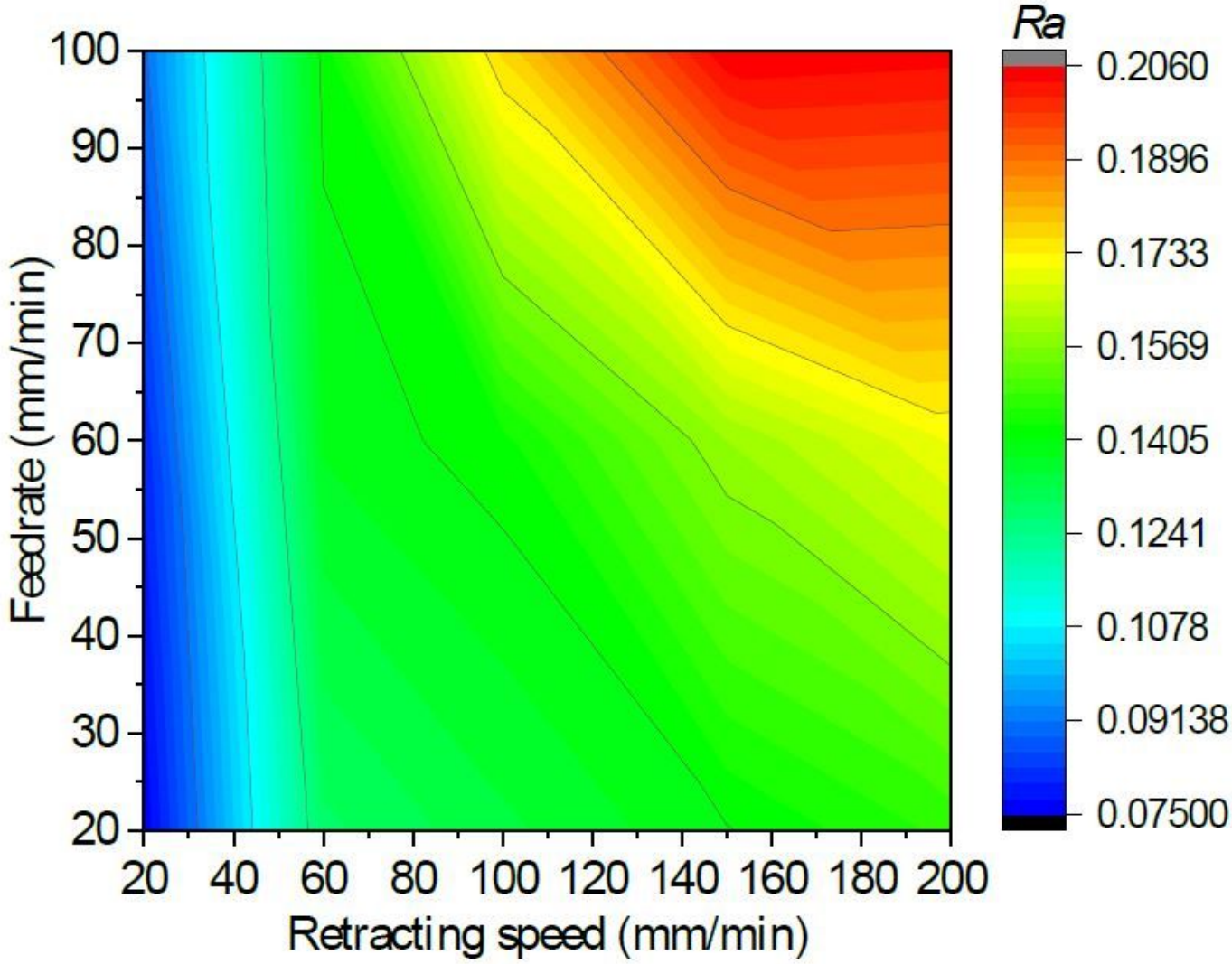

Figure 22

Contour map of Ra

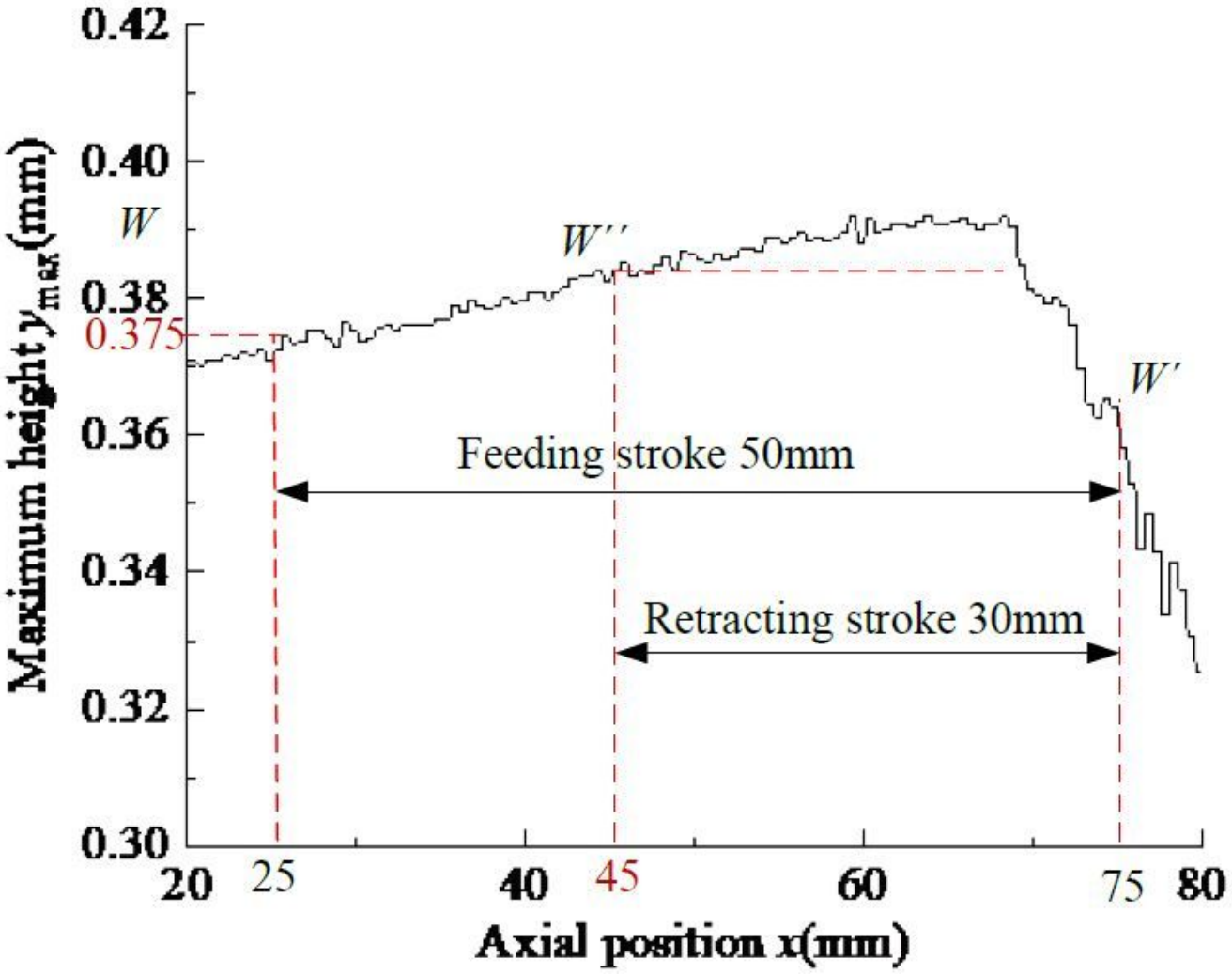

Figure 23

Schematic diagram of feeding stroke and retracting stroke